

Toward Real Setting Applications of Organic and Perovskite Solar Cells: A Comparative Review

Mirko Seri,* Francesco Mercuri,* Giampiero Ruani, Yaomiao Feng, Minzhang Li, Zong-Xiang Xu, and Michele Muccini*

The development of efficient, reliable, and clean energy sources is one of the global priorities for enabling a sustainable transition toward a green society and economy. The third-generation solar cells, such as organic solar cells (OSCs) and perovskite solar cells (PSCs), are among the most promising platforms for the generation of electrical power from sunlight for a wide range of applications. However, the widespread diffusion of emerging photovoltaics technologies is hampered by issues occurring in the translation of laboratory-scale R&D efforts to real settings. Herein, starting from a thorough survey of latest research on OSC and PSC technologies, critical factors related to fabrication and operation of solar cells, especially in terms of materials properties/requirements and beyond metrics built on efficiency only, are analyzed. On this basis, OSCs and PSCs are compared in terms of their potential in real application scenarios, also highlighting their peculiarities in view of their future large-scale utilization.

sustainable growth to reach a climate neutrality by 2050 (−55% CO₂ emissions compared with 1990, expected by 2030). To this end, the employment of fossil fuels, i.e., in the form of coal, oil, and gas, needs to be drastically reduced until replacement with new alternative and sustainable energy resources. Renewable energy sources are the most promising candidates because of their virtually endless availability, which could largely meet the global energy demand, with theoretically no impact on climate, environment, and human health.^[1] Moreover, they might have an economic advantage, because they can be produced at a competitive price, usually lower than fossil fuel-based generation, and have the potential to create millions of new jobs in the energy sector.

1. Introduction

The goal of an energy transition to fight climate change and its dramatic consequences on the environment are among the biggest challenges of the 21st century. With the European Green Deal, the EU aims at creating new strategies for a green and


As a possible solution, solar energy is a valid and promising alternative among renewables. Sun is a star, and its light is abundant (≈ 90 PW received on the earth's surface, almost four orders of magnitude higher than our annual energy consumption, ≈ 17 TW), inexhaustible (the sun will last for more than four billion years), and fairly well distributed over the planet. Solar energy, however, is not useful unless it is converted into final usable energy forms, such as heat and electricity. While conversion of solar energy into heat is relatively simple, the efficient conversion into electricity constitutes an important scientific and technological challenge. The rational development of photovoltaic (PV) technologies led to great improvements; however, new challenges are expected to arise if PV is to be massively deployed in our society. This depends on our capacity of constructing efficient, stable, scalable, cheap, versatile, adaptable, easily processable, and ecologically friendly PV devices based on abundant, accessible, and nontoxic elements/materials. Over the years, many different materials were used and developed for PV applications with the result of a wide range of technologies present nowadays. They can be classified in three generations depending on the maturity of the technology and different nature of the active materials used.^[2]

The first generation comprises commercially available systems and is typically associated with silicon. Silicon is one of the most abundant materials in the earth's crust and is suitable for PV applications because of its semiconducting properties and low bandgap of 1.1 eV. The derived technology (over 60 years old) uses wafers of silicon in crystalline (c-Si), single-crystalline (sc-Si), or multicrystalline (mc-Si) states with the first two

Dr. M. Seri
Istituto per la Sintesi Organica e la Fotoreattività (ISOF)
Consiglio Nazionale delle Ricerche (CNR)
Via P. Gobetti 101, 40129 Bologna, Italy
E-mail: mirko.seri@isof.cnr.it

Dr. F. Mercuri, Dr. G. Ruani, Dr. M. Muccini
Istituto per lo Studio dei Materiali Nanostrutturati (ISMN)
Consiglio Nazionale delle Ricerche (CNR)
Via P. Gobetti 101, 40129 Bologna, Italy
E-mail: francesco.mercuri@cnr.it; michele.muccini@cnr.it

Y. Feng, M. Li, Prof. Z.-X. Xu
Department of Chemistry
Southern University of Science and Technology
Shenzhen, Guangdong 518000, P. R. China

 The ORCID identification number(s) for the author(s) of this article can be found under <https://doi.org/10.1002/ente.202000901>.

© 2021 The Authors. Energy Technology published by Wiley-VCH GmbH. This is an open access article under the terms of the Creative Commons Attribution-NonCommercial-NoDerivs License, which permits use and distribution in any medium, provided the original work is properly cited, the use is non-commercial and no modifications or adaptations are made.

DOI: 10.1002/ente.202000901

typically consisting of rigid structures, whereas the latter is often mechanically flexible. The use of abundant and nontoxic elements, even though some components (e.g., connections and back sheets) still contain potentially dangerous elements/materials,^[3] in conjunction with the remarkable energy conversion efficiency and lifetime of the resulting devices, explains why silicon-based PV technologies are dominating the market. The number of locations where PV electricity is competitive with conventional technologies (e.g., coal or nuclear) is constantly increasing, and its portion of electricity production in some industrialized countries has become remarkable.^[1]

The second generation of PV accounts for technologies in early market deployment. It consists of thin-film devices based on inorganic semiconductors, such as amorphous (a-Si) and micromorph (μ -Si) silicon, cadmium telluride (CdTe), copper–indium–selenide (CIS), and copper–indium–gallium–diselenide (CIGS). Compared with the first generation, the use of thin films has several advantages, such as: 1) use of less material(s); 2) wider range of deposition methods for large-scale production; 3) relatively lower costs (related to materials and processing); and 4) specific characteristics (lightness, flexibility, semitransparency, etc.) enabling new application/integration possibilities. However, this generation suffers from issues of durability (a-Si), materials availability (In and Ga),^[4] and toxicity (Cd).^[5]

The third generation of solar cells includes emerging PV technologies at the pre-commercial stage, which still require further improvements/developments on specific aspects for real applications.

The last decades have witnessed a tremendous increase of the research efforts toward the development of the solar cells based on organic and hybrid (organic–inorganic) materials.^[6] The technologies applied to these novel kinds of PV systems rely largely on solution-processed methods, which are particularly useful for processing organic and macromolecular systems and nanoparticles.^[7] Alternatively, organic/hybrid (insoluble) small molecules and/or oligomers can be processed by thermal evaporation under vacuum conditions.^[8,9] At Heliatek GmbH, roll-to-roll (R2R) evaporated multilayer stacks of 10–20 nm films of organic molecules exhibited great performances, steadily gaining traction in architectural markets.^[10]

Clearly, the possibility of using a solution-based method to fabricate solar cell modules results in a number of advantages over traditional, solid-state manufacturing techniques, in terms, for example, of large-scale production or energy-related issues, as discussed in detail later.^[11]

Recent works demonstrated that most efficient systems for the development of novel PVs are based on either the organic solar cell (OSC) or perovskite solar cell (PSC) technologies. The peculiarities of these technologies suggest a huge potential in a wide range of fields, from large-scale energy production to special and/or unconventional applications.^[12]

The active component of OSCs is usually a blend of purely organic materials, such as small molecules or polymers. In contrast, PSCs involve the use of a hybrid system, commonly a hybrid organic–inorganic lead or tin halide perovskite as the light-harvesting active layer.^[13]

In this review, we focus the attention on these two emerging PV technologies, which offer a significant potential for new

applications and markets where their advantages and specific properties are fully valued. We report an overview on both technologies starting from their fundamentals, materials, and current state of the art and provide a discussion and comparison on the status and key aspects for real setting applications. The overall power conversion efficiency (PCE) of solar cells, defined as the portion of energy of the incoming sunlight that is converted into electrical power, is typically considered as the crucial performance figure of PV technologies. However, the real uptake of novel solar cell technologies is grounded by a complex interplay of a manifold of factors that should finally fulfill the main requirements to make OSCs and PSCs transferable from the laboratory research to the industrial context.

The comparative review that we propose aims to provide an overall picture on these emerging technologies to identify common aspects, distinguishing features, different key hurdles to be overcome, and potentially complementary applications. In light of this, OSCs and PSCs cannot be considered competitors but alternative complementary solutions for distinct conventional and unconventional application fields, thus strongly contributing to the supply of clean energy for a more sustainable future.

2. Organic and Perovskite-Based Solar Cells

2.1. Organic Solar Cells

2.1.1. Fundamentals

OSCs, because of their remarkable merits and unique properties, still represent one of the most investigated emerging PV technologies that could offer new and complementary opportunities and application areas compared with conventional PV technologies. Unlike other PV technologies, OSCs are based on photoactive π -conjugated organic molecules (or polymers) in which the presence of alternating C–C and C=C bonds creates a π -electron delocalization along the molecular backbone responsible for the resulting semiconducting properties.^[14] The chemical nature and the structural tunability of these materials, in combination with a relatively simple device architecture, offer to this technology a series of specific advantages and opportunities, summarized in the following, that motivate the huge interest and continuous research efforts.^[15]

Scalability at Low Cost: Solution-processable, environmentally stable, and relatively cheap organic semiconductors open the way to fast-printing techniques for the massive production of low-cost solar modules. Highly automated and R2R processing methods carried out under ambient conditions confer the further advantage of an economically sustainable production of OSCs with low material consumption.

Form Factor: Devices can be produced into many forms on flexible and lightweight supports. Solar panels can be rolled up, adapted on curved surfaces and/or on existing systems (e.g., building, objects, portable chargers, etc.) adding new functionalities.

Aesthetics and Transparency: The aspect of OSCs can be designed as a function to their final application or needs. As the main properties of organic materials can be tuned on purpose (via organic chemistry), the resulting OSCs can also

satisfy aesthetic requirements as color tunability, shape, and semitransparency or total transparency to meet specific applications (greenhouse, curtains, windows, decorations, etc.).

Harvesting Factor. OSCs provide an effective PV response at relatively low light illumination conditions. They offer, because of the high absorption coefficient of organic semiconductors, the capability to efficiently respond at the low light intensities (e.g., diffused or indirect light) and, almost indifferently, to different sunlight angles of incidence. This is a remarkable benefit not only because OSCs can provide a more constant power generation over the entire daily cycle (outdoor applications) but also because it allows unconventional indoor applications (windows blinds, windows, objects, portable chargers, etc.). Furthermore, the characteristic narrowed absorption of organic compounds (and its tailoring at specific wavelengths) can be exploited for additional applications such as the recycling of the light generated by light emitting diode (LED) lamps.^[16]

Environmental Profile. Organic compounds can be easily processed by solution, contain abundant, and nontoxic elements, and allow easy recycling of precious embedded materials, if necessary.^[17] OSCs have demonstrated an excellent sustainability profile in terms of energy pay-back time (EPBT) and carbon footprint.^[18] In particular, the use of mild conditions (both during material synthesis and device fabrication) and the further development of environmentally friendly processes represent a step forward in terms of sustainability and environmental impact of this technology.

Despite these remarkable advantages, OSCs still suffer significant limitations in terms of PCE on large scale (modules) and device stability, in particular, under harsh operating conditions, mainly related to thermal- and light-induced degradation.^[19] Nevertheless, the goal of the organic photovoltaic technology is not to reach or exceed the level of performance of more consolidated technologies, but it is to enable the fabrication of new devices that can provide smart solutions especially in application areas traditionally difficult for conventional PV systems. This represents a clear example on how different solar technologies can be complementary in terms of applications, thus exploiting the capability to convert light into energy in different but synergic ways.

The story of OSCs starts almost three decades ago and was characterized by important breakthroughs and “evolutionary steps” that boosted this technology toward the current state of the art.^[15]

The first PV devices were based on a single organic layer sandwiched between two electrodes having different work functions (WFs). The cells exhibited very low photovoltages with a PCE <0.1%.^[20] This was mainly due to the fact that organic materials, upon photoexcitation, generate tightly bound electron-hole pairs (Frenkel excitons) with a limited lifetime and a short diffusion length (<10 nm). Due to the low dielectric constant of organics (typically 2–4), these excitons require a much higher energy than the thermal energy (kT) to dissociate. For this reason, only excitons generated close to the electrode were able to dissociate, whereas all others generated in the bulk were lost through quenching processes.

To partially solve the problems of single-layer solar cells, Tang^[21] introduced, in 1979, the bilayer structure creating a planar heterojunction (PHJ) between two materials with different electron affinity (electron acceptor, A) and ionization potential

(electron donor, D). The frontier orbital energy offset at the D/A interface, larger than the exciton binding energy, was the key driving force for exciton dissociation: the electron was hosted by the acceptor (higher electron affinity), whereas the hole was hosted by the donor (lower ionization potential). The internal electric field (generated by the different WF of the electrodes) drives the free charges through the relative phases (reducing bimolecular recombination) toward the respective electrodes. However, the efficiency of bilayer devices was still limited by a low charges generation rate, mainly due to: 1) the limited exciton diffusion length in the D and A phases (<10 nm) and 2) the relatively low D/A heterojunction interfacial area available for excitons dissociation into separated charges, leading to recombination of the majority of excitons generated far from the D/A interface. Even though thinner layers would compensate the short diffusion length of excitons, the resulting losses in terms of optical absorption and, hence, exciton generation would not solve the problem.

A revolutionary breakthrough in organic PVs came in the mid-1990s with the introduction of the 3D heterojunction or bulk heterojunction (BHJ).^[22,23] This concept was introduced to address the limited exciton diffusion length of organic semiconductors, which was the main limiting factor of single-layer and PHJ solar cells. In a BHJ system, donor and acceptor materials are mixed together to form a bicontinuous interpenetrating network with large D:A interfacial areas and a phase segregation on the order of few tens of nanometers, allowing an efficient exciton diffusion and dissociation, thus yielding a significant improvement in terms of PCE. Being the scale of the blend comparable to the exciton diffusion length, the exciton quenching is drastically limited, because in the proximity of each photogenerated exciton, there is an interface with the acceptor able to favor exciton dissociation, even for relatively thicker active layers (>100 nm). Hence, charge generation takes place in a 3D D:A interface homogeneously distributed within the active layer. Provided that bicontinuous pathways (n-type and p-type) exist in each material from the interface to the respective electrodes, the photon-to-electron conversion efficiency is dramatically increased. Since then, the BHJ structure became the standard approach for OSCs.

In parallel, the efficient photoinduced electron transfer from a conjugated polymer to fullerene (C₆₀) discovered by Morita et al.^[24] and Sariciftci et al.^[25] started the era of fullerene derivatives as new acceptor materials, in combination first with poly(2-methoxy-5-(2-ethylhexyloxy)-1,4-phenylenevinylene) (MEH-PPV) and poly(3-hexylthiophene-2,5-diyl) (P3HT), and then with a huge variety of donors. Indeed, the great electron delocalization properties of fullerenes, which results in a suitable electron affinity, the great electron mobility, and the possibility to obtain fullerene derivatives soluble in organic solvents ([6,6]-phenyl C₆₁ (or C₇₁) butyric acid methyl ester [PCBM]), make PCBM as one of the most suitable and used n-type materials for BHJ devices. Polymer-fullerene systems dominated the field of high-efficiency OSCs for the last decades even though the recent introduction of nonfullerene derivatives, as discussed later, represents a new promising frontier offering more stable and efficient devices, highlighting the possibility of further remarkable progress.

A typical devices structure of a BHJ solar cell is reported in **Figure 1A**. It consists in a multilayer stack based on: a glass

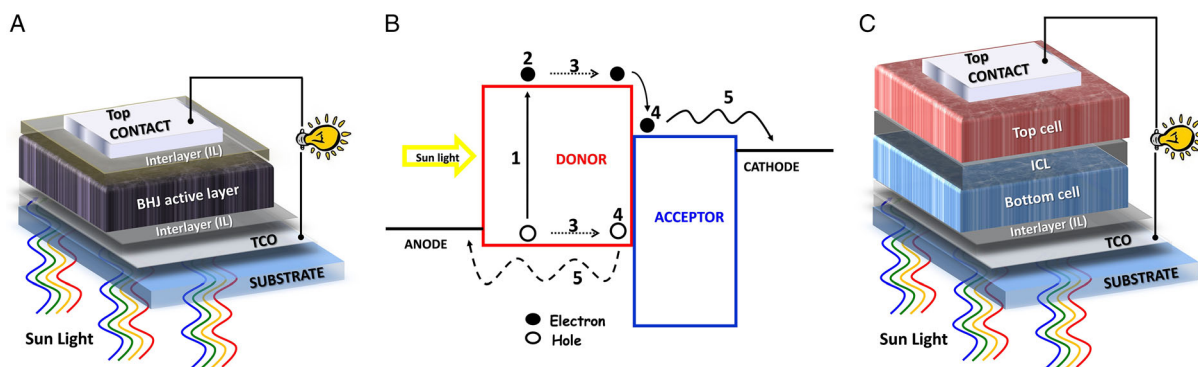


Figure 1. A) Device structure of a single-junction OSC, B) schematic representation of the working mechanism within a BHJ device, and C) device structure of a tandem solar cell.

substrate (rigid or flexible) covered with a transparent conductive oxide (TCO; e.g., indium-tin-oxide [ITO]) acting as electrode, a carrier selective layer (interlayer [IL]), a D:A (BHJ) blend, a second carrier selective layer (IL), and a top electrode (usually a metal, thermally sublimated).

This device can adopt a standard or inverted configuration, depending on the “direction” of photogenerated electrons and holes. The difference arises from the choice of proper IL/electrodes and subsequent polarization. In a standard (inverted) configuration, the bottom electrode, ITO, acts as anode (cathode), whereas the top contact acts as cathode (anode). Each electrode is properly combined with selective IL (hole-transporting layer (HTL) and electron-transporting layer (ETL) for anode and cathode, respectively) to optimize the charge extraction/collection, as discussed in the next section. Compared with standard structures, inverted cells not only offer identical performances but also exhibit enhanced stability/lifetime due to the use of high WF metals (Ag, Au, Cu, etc.), more stable against oxidation, as top anode.^[26]

A single-junction architecture, despite the great progresses and results, is intrinsically limited in performances by two main energy loss pathways: 1) transmission losses, when photons with energy lower than the bandgap pass through the blend without absorption, and 2) thermalization losses, when photons with higher energy than the bandgap are absorbed generating a highly excited state, which relaxes into a lower excited state by releasing the surplus energy as heat. These losses can be alleviated with two (or more) absorber materials or layers. Two promising approaches are the use of more complex ternary or tandem structures (both standard or inverted), where two different donor materials with complementary absorption spectra (in combination with an acceptor) are mixed together in a single-layer device (ternary: D1:D2:A)^[27] or used as two individual active blends (D1:A and D2:A) of subcells connected in a multijunction configuration (tandem, see Figure 1C).^[28] In particular, a wide bandgap blend is typically used in the bottom cell (to reduce thermalization losses), whereas a low bandgap layer is used in the top cell (to reduce transmission losses). The two subcells are electrically connected by an interconnecting layer (ICL), which is one of the critical issues of solution-processable tandem cells, because it should simultaneously fulfill several specific requirements (ease of processability, robustness, stability, transparency, energy

alignment, high conductivity, etc.).^[29] Regardless of the device architecture, the fundamental physical processes within a BHJ blend/device, allowing the conversion of photons to electric charges, are schematically represented in Figure 1B. Interested readers can find detailed information on dedicated review articles.^[30,31]

The conversion mechanism is based on five consecutive steps, briefly described hereafter.

1) *Light irradiation and photon absorption:* The first process occurring in a solar cell is the incidence of the sun light on the device, allowing photons to reach the BHJ blend. However, before reaching the active compounds, the sunlight passes through other materials/layers, which must ensure an optimal transparency (avoiding reflection and/or scattering effects). Upon reaching the active layer, an efficient photon absorption process can occur, depending on: 1) the overlap between the BHJ absorption spectrum (in particular, that of the donor being the material with lower bandgap) and the spectral solar emission and 2) the absorption intensity at each wavelength, ruled by the Lambert–Beer law, where the absorbance linearly depends on the optical density of the film (correlated with the molar extinction coefficient, the mass density of the layer, and the orientation of absorbing molecules) and on its thickness. Note that, a good balance between film thickness and its charge transport capability should be considered to optimize the device performance.

2) *Exciton generation:* The generation of an electron–hole pair, by photoexcitation of an organic material, results in an excited but neutral state with a limited and finite lifetime; this state is termed exciton (Frenkel exciton) and consists of a strongly bound and localized electron–hole pair (binding energy around 0.3–1 eV), as a consequence of the weak intermolecular interactions and low dielectric constant typical of organic molecules.^[30] The system can deactivate again to the ground state S_0 , radiatively (fluorescence) or thermally (internal conversion), or via triplet states (T) (intersystem crossing and vibrational conversion).

3) *Exciton diffusion:* This is typically an energy transfer processes, which can occur through two different ways: Förster (long range) or Dexter (between adjacent molecules) transfers can take place between an excited molecule (considered as excitation donor) and a molecule that receives the excitation.^[30] This quasiparticle diffuses inside each material phase as long

as recombination or splitting processes do not take place. The recombination or splitting pathways strictly depend on the balance between the nanoscale dimension of the D:A phase separation and the exciton diffusion length.

4) *Exciton dissociation*: If the exciton diffusion length is sufficient to meet an internal field (D:A interface), hole and electron separation can occur. Indeed, if the energy difference between the ionization potential of the donor (D) and the electron affinity of the acceptor (A) is larger than the exciton binding energy, exciton dissociation is energetically favorable. However, the dissociation step passes through an additional intermediate state called charge transfer (CT) state where the two “charges” are localized in two different phases but are still “bound” by their mutual Coulomb attraction. An additional force, typically imposed by the different WF’s of the electrodes, is needed to split the charges. Note that, tightly bound CT states may also represent a possible loss channel because of geminate recombination (transition from the CT state to the ground state).

5) *Charge transport*: Once the charges are generated, holes can diffuse in the p-type material, whereas electrons can move in the n-type phase. In disordered organic semiconductor thin films, charge transport occurs via hopping of charge carriers between transport sites within the density of states. The internal built-in electric field within the device drives the generated-free charge toward their respective electrodes. The selection of D:A materials and, in particular, the nanoscale morphology of the BHJ blend play a crucial role for the charge transport. Indeed, molecular packing (intermolecular distances), D:A domain dimensions, length, and continuity of the domain paths are determining factors not only to optimize the charge mobility but also to avoid charge recombination, one of the main loss channels for state-of-the-art solar cells.^[32]

The last step of the PV process consists in the charge collection at the electrodes (in contact with an external circuit). The main requirements are: 1) the choice of materials with suitable conductivity as electrodes (e.g., metal and conductive polymers) and 2) the need for “ohmic” contacts at the active layer/electrode interfaces. Often, the use of ILs with suitable energy levels is adopted to improve the ohmic contacts, thus avoiding charges accumulation and, furthermore, improving the charge selectivity through the suppression of bimolecular recombination at low electric fields (see the next section).

2.1.2. State of the Art

To date, the continuous development and fine optimization of innovative active and functional materials, device structure, processing conditions, and the understanding of film morphology and device physics led to the state-of-the-art polymer solar cells with PCEs (on laboratory scale) up to 18%,^[33] significantly reducing the gap with other emerging PV technologies. As mentioned earlier, despite the promising results and the increasing trend in terms of PCE after the introduction of new emerging materials, this technology still requires further efforts for real applications, mainly focused on device upscaling and lifetime/stability. This might allow to fully exploit the huge potential of OSCs to spread into a wide range of end-use areas with a significant market penetration, not only limited to niche applications and/or smart integrations where other technologies cannot be used.

It is generally accepted that a mature PV technology reaches 60–80% of the laboratory record PCE.^[34] This difference is commonly defined as *scaling gap* and includes, in particular, for OSCs, additional aspects such as the simplification of the donor/acceptor chemical structures (with a reduced number of synthetic steps, high yields, amount, and toxicity of solvents) and compatibility of the module fabrication procedure with industrial standards. To this end, it is of crucial importance to investigate the challenges associated with the process issues for large-area OSC manufacturing and their impact on the resulting module performance.

Several recent studies and results, highlighting the performance evolution of organic “mini-modules” (>1 cm²), are briefly reported. Two representative examples of organic solar modules are reported in **Figure 2**.

In 2016, Hong et al.^[35] reported a certified PCE of 7.5% for an organic mini-module (4.15 cm²) based on poly [4,8-bis(5-(2-ethylhexyl)thiophen-2-yl)benzo[1,2-b:4,5-b']dithiophene-2,6-diyl-alt-(4-(2-ethylhexyl)-3-fluorothieno[3,4-b]thiophene)-2-carboxylate-2,6-diyl] (PC71BM and PTB7-Th). In 2018, Zhang et al.^[36] demonstrated a remarkable PCE of 8.6% (uncertified), with a fill factor (FF) of 65%, for a nonfullerene acceptor (NFA)-containing module (3.48 cm²) based on five cells connected in series. In 2015, Mori et al.^[37] showed an organic photovoltaic (OPV) module with PCE = 9.7% (26 cm²), claiming scalability to even larger modules.

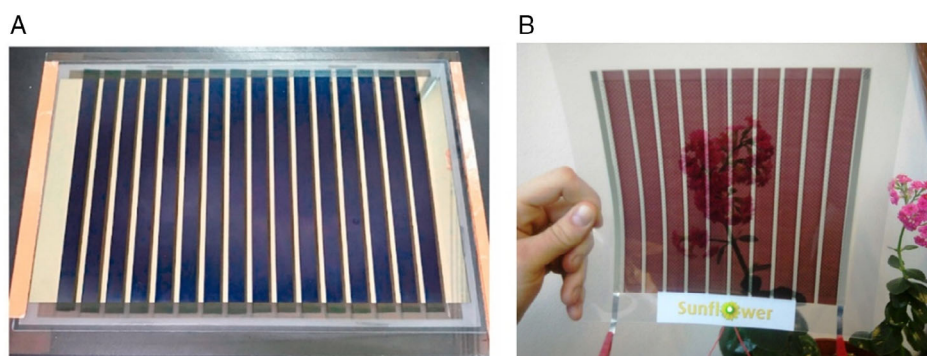


Figure 2. Images of OSC modules fabricated either by blade coating on rigid glass A) 30 cm × 20 cm, or by printing on mechanically flexible plastic substrates B) 20 cm × 20 cm. A) Adapted with permission.^[39] Copyright 2020, Elsevier. B) Adapted with permission.^[29] SUNFLOWER, EU project n. 287594.

Recently, Facchetti and co-workers^[38] reported a (relatively) large-area module (a total dimension of $\approx 81 \text{ cm}^2$ and an active area of $\approx 30 \text{ cm}^2$) with a record PCE of 10.4% (10.1% certified) using a nonfullerene-based blend processed from unchlorinated solvents. Moreover, compared with analogous laboratory-scale devices (a PCE of $\approx 13\%$) the presented module exhibited only a $\approx 20\%$ cell-to-module loss (scaling gap), representing an important step forward in the development of large-scale OPV modules. In 2020, Tsai et al. reported a blade-coated organic-based module series-connected ($30 \text{ cm} \times 20 \text{ cm}$) with an active area of 216 cm^2 and a PCE of 9.5% with a V_{OC} of 13.5 V (reported in Figure 2A).^[39]

Concerning device stability, another key point for a large commercialization, a huge number of studies investigate the possible degradation mechanisms occurring in OSCs. However, the volume of research undertaken to better understand this process is still smaller than that oriented to the further enhancement of device PCE. Typical degradation pathways include, for instance, photochemical reactions of organic components (e.g., within the BHJ blend), the oxidation/delamination of electrodes, intrinsic/interfacial instability of ILs, and possible failure of device encapsulation. This represents only a small part of the complex and interlinked phenomena responsible for device degradation. A detailed discussion on this topic can be found in several comprehensive reviews.^[19,40] Interestingly, Brabec and co-workers proved an NFA-based OSC with predicted lifetime approaching ten years.^[41] More recently, Forrest and co-workers demonstrated an extremely stable evaporated single-junction OSC with a predicted lifetime of up to 9.3 years.^[42] These results, even if carried out in indoor conditions, show that the OSCs based on nonfullerene materials are very promising in terms of stability.

Despite the great advantages and remarkable merits of OSCs, they still cannot reach the level, in terms of costs/benefits, of the more consolidated silicon technology, which, having a similar cost of acquisition, offers greater performance both in terms of efficiency and lifetime. Nevertheless, it is clear within the research community that the application potential of OSCs could be fully deployed upon further investigation and optimization of the current drawbacks and limitations. This indeed might explain why several companies are commercializing organic PV products/solar panels (e.g., infinityPV, ARMOR/OPVIUS, Eight19, Solarmer Energy, Sunew, Heliatek, etc.), and numerous researchers still dedicate lot of efforts to fundamental studies regarding degradation mechanisms, performance optimization, and scale-up processes, continuously enhancing the state of the art and generating a precious know-how to enable the deployment of the full application potential of OSCs.

2.2. Perovskite Solar Cells

2.2.1. Fundamentals

Hybrid metal halide PSCs experienced an extremely rapid development that, in a few years, brought these devices to compete in conversion efficiency with single-crystal Si solar cells. The high efficiency (up to 25.5%)^[43] together with the low temperature and relatively low cost processes required for the fabrication of PSCs attracted the interest of many research groups worldwide.

ABX_3 represents the general formula of perovskites: in hybrid perovskites, investigated in solar cells, A is the cation (methylammonium CH_3NH_3 , formamidinium (FA) $\text{HC}(\text{NH}_2)_2$, or cesium), B is a divalent metal (Pb, is the one that, to date, gives higher performances), and X is a halide ion (I, Cl, and Br).

The physical properties of hybrid perovskites make this class of materials striking for many optoelectronic devices, not only for solar cells, but also for high-performance LEDs.^[44]

The main distinguishing characteristics of hybrid perovskites are: 1) low electron and hole effective masses^[45]; 2) high carrier mobility of both electron and holes ($13\text{--}15 \text{ cm}^2 \text{ V}^{-1} \text{ s}^{-1}$);^[46] 3) long carrier lifetime (on the order of tenths of μs);^[47] 4) high charge carrier diffusion length ($> \mu\text{m}$)^[46]; 5) ambipolar behavior with good charge carrier separation; 6) tunable direct bandgap (1.47–2 eV);^[48] 7) large absorption coefficient ($1.5 \times 10^5 \text{ cm}^{-1}$);^[48] 8) high dielectric constant (60 at low frequency);^[49,50] and 9) low exciton binding energy (few meV).^[45]

While the large absorption coefficient of perovskites ensures the possibility to work with thin active films, low exciton binding energy, high dielectric constant, high mobility, long lifetime, diffusion length of charge carriers, and ambipolar behavior of perovskites are the essential ingredients for an efficient generation, transport, and collection of photogenerated carriers at the electrodes of the solar cells. The tunability of the direct bandgap allows both to obtain relatively large V_{OC} and to select the best optical absorption range for application in tandem cells configuration. The possibility to build hybrid perovskites by changing or mixing different elements is one of the key aspects that make this class of materials particularly relevant both for improving the light-to-electricity conversion efficiency and for increasing the lifetime of PV devices by tuning their physical and chemical properties.

The ambipolar behavior of hybrid perovskites represents the principal distinguishing characteristic of this system, and the dynamics of charge carriers in PSCs is one of the key factors that determine their high performances. To date, a unified interpretation of the possible dominating mechanisms ruling the charge carrier dynamics in PSCs is still missing, and we, therefore, recall here some of the proposed models.

The large spin–orbit coupling associated with the presence of heavy metals (e.g., Pb) brings the electronic levels to Rashba–Dresselhaus splitting of band edges and, as a consequence, to a reduced charge recombination.^[51,52]

Frost suggested that the long lifetime of photogenerated carriers could be associated with the presence of ferroelectric phase at operating temperatures related to efficient charge separation due to strong lattice polarization such as in ferroelectric phase.^[53] To date, evidences of ferroelectric phases in hybrid metal halides perovskites have been observed only well below the room temperature.^[54] Two types of mechanisms related to electron–phonon coupling have been proposed to determine the charge dynamics in hybrid perovskites: a Fröhlich type polar interaction where electrons are coupled to the electric field generated by the polarization of the lattice^[55] and the interaction of photogenerated carriers predominantly with acoustic phonons (deformation potential).^[56] Several mechanisms associated with the presence of polarons in hybrid perovskites have been proposed to explain the charge transport properties in these materials.^[53,57–63] In highly polarizable materials, it is common to consider the

presence of quasiparticles such as polarons formed by the charge carriers and the local deformation of the lattice around the carrier itself. In the case of large polarons in hybrid perovskites, the repulsion between opposite charges is calculated to be stronger than the Coulomb attraction, leading to the reduction of the recombination process.^[64] Also, ab initio calculation has shown the confinement of electrons and holes in spatially separated domains, accounting for the low recombination of photogenerated carriers.^[65] Hybrid perovskite films are grown by wet deposition processes (spin coating, slot-die coating, and screen printing) or thermal evaporation. Spin coating, either in a single step or two steps, followed by a relatively low temperature annealing ($\approx 100^\circ\text{C}$) is the more diffuse deposition technique for hybrid perovskite films, for its ease of use and low cost. In single-step processes, all precursors are dissolved together in a single solution,^[66] to drip onto the substrate and spun (quality of the deposited films can be improved by anti-solvent methods).^[67,68] In the two-step sequential deposition method, the metal halide (e.g., PbI_2) film is first deposited by spin coating, and then, a second solution containing the organic cation such as $\text{CH}_3\text{NH}_3\text{I}$ (MAI)^[69] is deposited to favor an interdiffusion growth process.^[70]

Hybrid perovskite films have also been deposited using a dual-source thermal evaporation,^[71] leading to films with better control in thickness and with less pinholes than those deposited by solution techniques. However, the relatively higher complexity of the method limits its use. Sequential layer-by-layer vapor deposition or combined wet/vapor deposition is an additional option for hybrid perovskite film deposition (for more details, see the previous study^[72]).

Hybrid perovskites have been initially introduced as a dye in the quantum dot-sensitized solar cells.^[73] The further step was to infiltrate the mesoporous TiO_2 layer filling the empty spaces (not

only decorating the surface of the transparent semiconductor) with the $\text{CH}_3\text{NH}_3\text{PbI}_3$ (MAPbI) hybrid perovskite^[66] exploiting the capability of this material not only to photogenerate charge carriers, but also to efficiently transport both positive and negative charges. This was the beginning of a rapid conversion efficiency improvement that, in a few years, brought this class of materials to be the most intriguing and attractive one in the PV technologies scenario. The architecture of this kind of cells (Figure 3) is the following: a compact layer of TiO_2 on top of the photoanode (fluorine doped tin oxide [FTO]), together with the mesoporous TiO_2 layer, acts as a hole blocking layer and collects the electrons; the hybrid perovskite is deposited to fill the pores of the mesoporous structure and is covered with an electron blocking layer (usually doped spiro-2,2',7,7'-tetrakis[N,N-di(4-methoxyphenyl)amino]-9,9'-spirobifluorene [OMeTAD]) letting holes to reach the electrode (evaporated or painted as final element of the cell). The presence of a mesoporous component requires annealing temperatures on the order of 450°C , restricting drastically the number of suitable substrates. The introduction of planar configurations^[74] opened the possibility to use different photoanodes (light, flexible, etc.) as well as to use inverse (n-i-p) configuration with respect to the standard p-i-n one (Figure 3).

2.2.2. State of the Art

The possibility to tune the composition of the perovskite together with the selection of proper interface materials as well as the introduction of physicochemical treatments for reducing point and extended structural defects brought both the efficiency and the stability of PSCs to a continuous increase.

The highest certified conversion efficiency of a perovskite-based solar cell, reported by the National Renewable Energy Laboratory (NREL, which keeps track of the advances of certified

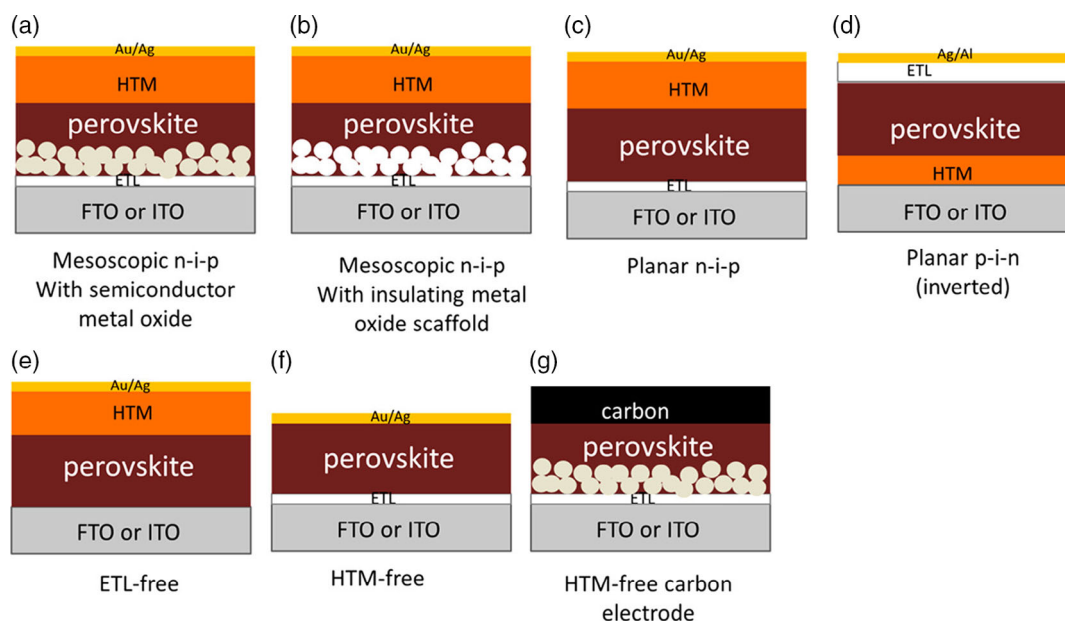


Figure 3. Schematics of various perovskite-based solar cell architectures. a) mesoscopic n-i-p with semiconductor metal oxide; b) mesoscopic n-i-p with insulating metal oxide scaffold; c) planar n-i-p; d) planar p-i-n (inverted); e) ETL-free; f) HTM-free; g) HTM-free carbon electrode. Adapted with permission.^[291] Copyright 2019, American Chemical Society.

results in PVs), is 25.5% obtained by the Korean research center Ulsan National Institute of Science and Technology.^[43]

The Helmholtz–Zentrum of Berlin (HZB) brought the conversion efficiency record of perovskite-silicon tandem solar cells to 29.15%.^[75] In view of the compatibility of the deposition processing of perovskite devices with conventional 156 mm × 156 mm silicon bottom solar cells, coupled to the high conversion efficiency and the stability, PSC-Si tandem cells are considered to be the perovskite-based PV cells, which are closest to commercialization.^[76,77]

As far as modules are concerned, it is noteworthy to highlight the result of Panasonic that reached 16.09% conversion efficiency in a 30 cm × 30 cm single-junction module using a hybrid perovskite active layer deposited by inkjet coating technology (Figure 4).^[78]

High efficiency and relatively long-term stability in PSCs have been obtained following different strategies: improving the deposition conditions;^[79] introducing an organic ionic solid additive into the perovskite active layer;^[76] and efficiently encapsulating devices. At the moment, a one-year outdoor test on graphene encapsulated PSC panels is carried out in Crete within the EU's Graphene Flagship program. A marketable solar cell will need a lifetime larger than 20 years, which, in a laboratory scale, corresponds to a PCE decrease smaller than 10% after 1000 h of accelerating aging test. Even more aggressive accelerating aging tests—corresponding to 50 years of testing—working at 85 °C under 5 sun illumination have been proposed for better evaluation of the stability/degradation conditions of the devices.^[80]

However, stability reported in scientific literature is evaluated in the timescale of hours (300–10 000 h) that means—according to equivalent aging time of the experimental condition used—from few days up to few years.

Indeed, the most limiting factor of PSCs is the instability of the system. Relative humidity, heat, and UV light exposure induce the activation of degradation processes of the perovskite-based solar cells mostly acting on the perovskite itself.^[80]

To overcome this problem, many strategies are used: substitution (or partial substitution) of methylammonium (MA) with the larger organic cation FA,^[81,82] and/or inorganic, such as

Cs;^[83] introducing 2D/3D perovskite junctions and removing the HTL^[84] use of stable undoped hole conducting materials for preventing dopant migration toward the interface;^[85] and passivation of the surface, grain boundaries, and point defects.^[86]

Another limiting factor for perovskite-based solar cell commercialization is related to the instability of the solution precursors that makes the morphology of the perovskite film and, consequently, the devices performances, strongly dependent on solution aging.^[87]

3. Materials

Active and functional materials are the key enablers of next-generation PV technologies.^[88] As it will be shown in the following, the properties of individual materials used for the fabrication of solar cells determine crucially the potential of OSCs and PSCs in real setting applications.^[89–91] Essentially, all materials properties, from the molecular scale to the macroscale, are intertwined with the complex phenomena underlying the working mechanism of solar cells.^[92,93] The PCE is strongly affected, among other factors, by the type and quality of photoactive materials used: the right choice of materials can bring us closer to the thermodynamic performance limit. Other functional materials (ILs, charge transport, blocking, and injection/collection layers) need specifically tailored properties to fulfill some strict requirements for sustaining the overall performance figures.^[94,95] However, the development and fabrication of novel materials are usually complex, costly, and time-consuming. The complexity of the relationship between structure and functionality in working environments hinders the rational design of new materials for PVs. Moreover, materials with excellent properties at the laboratory scale or in the fabrication of prototypes can result completely inadequate for large-scale production of solar cell modules in terms of fabrication cost, efficiency, availability of raw materials, stability, toxicity, and several other aspects.^[96,97] The connection between materials properties and their potential in the development of OSCs and PSCs must carefully be assessed to improve the technologies beyond trial-and-error approaches. The development and engineering of novel materials for PVs

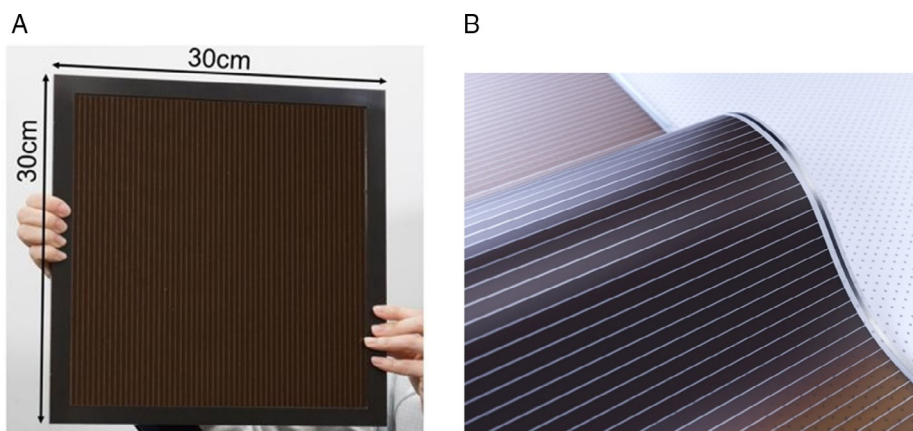


Figure 4. A) The Panasonic perovskite-based solar panel with the world's highest energy conversion efficiency. Adapted with permission.^[78] Copyright 2020, New Energy and Industrial Technology Development Organization (NEDO). B) Flexible PSC panel produced by Saule Technologies. Adapted with permission.^[296] Copyright 2020, Saule Technologies.

applications, together with device engineering, are, therefore, considered as the most crucial aspects for the advancement in solar cell technologies.^[98–100] In the following section, the main features of materials for OSCs and PSCs, in terms of their function, properties and performance, and in the context of scale-up applications, are discussed.

3.1. Photoactive Materials

3.1.1. Organic Photoactive Materials

Organic semiconductors are carbon-based π -conjugated molecules or polymers. The possibility to “easily” synthesize and manipulate their chemical structure is the real added value of these materials, offering the great advantage to finely tune the resulting properties to meet specific requirements and/or constrains for fabrication of innovative optoelectronic devices. Indeed, when key structural requirements are met, these materials and the resulting devices are able to simultaneously exhibit unique properties with optimal performance. However, a fundamental understanding of the delicate structure–property relationship as well as the strategic synthetic routes are of extreme importance to generate improved materials, justifying the extended research efforts over the last decades.^[101]

Many different requirements need to be simultaneously fulfilled by organic semiconductors for their application in OSCs. Indeed, besides very important energetic constrains for device application, these materials should simultaneously provide: good environmental stability, broad optical absorption (suitable bandgap), high absorption coefficient, proper solubility in different solvents, high charge mobility, thermal/light stability, and good film-forming capability.

To fulfill all these requirements, a huge library of electron donor materials (polymers and/or small molecules), because of their easier chemistry and much higher degree of freedom in terms of new design/functionalization compared with PCBM (acceptor), have been prepared and characterized during the last decades. The development of donor polymers has gone through several phases of research.

Three early classes of polymers should be mentioned, being the workhorses for several years and still representing effective benchmark materials: 1) PPV derivatives, such as MEH-PPV and poly(2-methoxy-5-(3',7'-dimethyloctyloxy)-1,4-phenylenevinylene) (MDMO-PPV); 2) poly(thiophene) derivatives (e.g., P3HT); and 3) polyfluorene (PF) derivatives such as poly([2,7-(9,9'-dihexylfluorene)]-alt-[4,7-di(thiophen-2-yl)benzo[c][1, 2, 5]thiadiazole]) (PFDTBT).

In 1995, Heeger and co-workers^[22] reported the first BHJ device based on MEH-PPV and PC₆₁BM as donor and acceptor materials, respectively. To further enhance the polymer processability and the resulting BHJ nanoscale morphology, the alkyl side chains of MEH-PPV were replaced with longer ones (MDMO-PPV) that, without altering the electronic properties of the polymer backbone, led to BHJ solar cells with PCEs \approx 3%.^[102]

To pursue higher efficiency, the research focus quickly shifted to soluble polythiophenes, especially regioregular P3HT, based on the repeating substituted thiophene units, which initially showed device PCEs of \approx 3% in BHJ solar cells.^[103,104] Nevertheless, the interest for this polymer mainly arose from

its relatively low bandgap (1.9 eV) and high aggregation tendency (semicrystalline character) at the solid state, thus rapidly becoming the most investigated and popular material for OSCs in the 2000s. Moreover, morphological optimization of P3HT-based blends led to BHJ devices with PCEs up to \approx 5%, thus attracting worldwide interests in OSCs.^[105] With the introduction of NFAs, the P3HT:NFA-based devices have recently reached PCEs up to 9.5%.^[106] To date, P3HT is still one of the benchmark materials for numerous studies, helping to unravel structure–property relationships and device engineering methods for other high-performance polymers.

The third major class of donor polymers for OSCs is represented by PFs.^[107] The most common PF derivatives contain fluorene and benzothiadiazole (BT) moieties, opportunely functionalized, as repeating units in the polymer backbone. In 2003, Andersson and co-workers^[108] first reported the PFDTBT polymer composed of fluorine and dithienyl-BT (DTBT) moieties with a bandgap of 1.9 eV and a highest occupied molecular orbital (HOMO) of -5.7 eV. Though V_{OC} was high (1.04 V), solar cells prepared from PFDTBT:PC₆₁BM showed a PCE of 2.2%, mainly limited by the low current generated. Later, through an alkyl chain modification of PFDTBT and device processing optimization, the resulting polymer PF10TBT led to BHJ solar cells with a PCE of 4.2%, with an almost doubled photocurrent compared with PFDTBT.^[109]

Although PPV, polythiophene, and PF derivatives played a significant role in the development of OSCs, one major limitation concerns the partial absorption of incident photons by the active blend due to a narrow bandwidth of its absorption spectrum. One of the most common methods to enhance the spectral absorption of a semiconductor is the reduction of its bandgap by molecular engineering.^[110]

The state-of-the-art polymer semiconductors for OSCs are donor–acceptor (D–A) conjugated copolymers, which consist of at least two alternating moieties along their backbone: an electron-rich donor (D) and an electron-deficient acceptor (A). Unlike homopolymers, with only one moiety such as P3HT, the D–A copolymers offer the great advantage of flexible tuning of the energy bandgap and energy levels. Specifically, the resulting HOMO and lowest unoccupied molecular orbital (LUMO) energy levels are largely determined by the HOMO energy of the donor unit and the LUMO energy of the acceptor unit, respectively, whereas the bandgap is mainly related to the strength of the electron-pushing (and withdrawing) abilities of the donor (and acceptor).^[111]

This effective approach allowed the design and synthesis of a huge library of semiconducting copolymers (large, medium, and low bandgap) with enhanced performance based on a wide number and variety of electron-rich and -deficient building blocks. Consistently with the goal of this review, we will provide a brief overview just on some of the most representative building blocks/monomers for efficient donor copolymers. Comprehensive reviews on this topic can be found elsewhere.^[112]

BT and DFBT Units: BT and its derivatives are largely used as electron-withdrawing building block for the synthesis of polymer for PV applications.^[113] The first copolymers, poly[2,6-(4,4-bis-(2-ethylhexyl)-4H-cyclopenta[2,1-b;3,4-b']dithiophene)-alt-4,7(2,1,3-benzothiadiazole)] (PCPDTBT), were based on the combination of BT with the electron-rich cyclopenta[2,1-b;3,4-b]dithiophene (CPDT).^[114] Optimized devices afforded PCEs up to 5.5%.^[115]

A fine structural tuning on the CPDT unit was carried out, in particular, replacing the carbon atom on the cyclopentane portion with Si or Ge.^[116,117] Interestingly, the presence of heteroatoms did not modify the bandgap of the polymers, but led to more ordered domains within the BHJ yielding optimal device performance without the use of solvent additives as in the case of the analogous carbon-based structure (PCPDTBT).

A further modification on the cyclopentane ring of the CPDT unit was carried out by adding an oxygen atom, thus creating an asymmetric moiety, dithieno[3,2-*b*:2,3-*d*]pyran (DTP). The combination of a DTP unit with the fluorinated BT (difluorobenzothiadiazole [DFBT]) generated the efficient low bandgap polymer poly[2,7-(5,5-bis-(3,7-dimethyl octyl)-5H-dithieno[3,2-*b*:2',3'-*d*]pyran)-alt-4,7-(5,6-difluoro-2,1,3-benzothiadiazole)] (PDTP-DFBT). BHJ solar cells based on PDTP-DFBT afforded PCEs up to 8%, showing the high V_{OC} and J_{SC} values.^[118]

DFBT was also combined with differently functionalized thiophene units to form a series of polymers. Among them, the polymer PffBT4T-2OD in combination with PC₇₁BM, through specific high-temperature processing conditions, led to a single-junction solar cell with a PCE of 10.8% and an FF of 77%.^[119]

DPP Units: The diketopyrrolopyrrole (DPP) unit has a well conjugated structure with strong π - π interactions and electron-withdrawing effects, largely used for preparation of low-bandgap D-A polymers. The potential of soluble DPP molecules and polymers has been explored with remarkable results in OSCs.^[120] One of the first polymers containing a DPP and three thiophene rings unit was poly[2,2'-((2,5-bis(2-hexyldecyl)-3,6-dioxo-2,3,5,6-tetrahydropyrrolo[3,4-*c*]pyrrole-1,4-diyl)dithiophene)-5,5'-diyl-alt-thiophen-2,5-diyl] (bandgap of 1.3 eV), able to harvest a light of up to 930 nm and yield BHJ devices with PCEs of \approx 6%.^[121] Combining DPP with thienyl-substituted benzodithiophene (BDTT), to form poly(2,6'-4,8-di(5-ethylhexylthienyl)benzo[1,2-*b*:3,4-*b*]dithiophene-alt-5,5'-dibutyloctyl-3,6-bis(5-thiophen-2-yl)pyrrolo[3,4-*c*]pyrrole-1,4-dione) (PBDTT-DPP), it was possible to reach PCEs greater than 6%.^[122]

By additional structural modifications on PBDTT-DPP, replacing the carbon atom on the thiophene spacers with selenium was possible to prepare PBDTT-a Se-based derivative, which, in combination with PCBM, led to solar cells with PCEs of 7.2%.^[123] Other notable DPP polymers in recent years include polymers-based DPP linked to thieno[3,4-*b*]thiophene (TT) units. As a result, a series of DPP and TT based polymers, also including the presence of heteroatoms in their structures, led to BHJ devices with PCEs approaching 9% and impressive J_{SC} s up to 23.5 mA cm⁻².^[124]

TT Units: In 2009, TT units were introduced as a strong acceptor building block for preparation of efficient donors.^[125,126] TT units were combined with the differently functionalized benzo[1,2-*b*:4,5-*b*]dithiophene (BDT) moieties, giving a series of copolymers with the bandgaps of \approx 1.6 eV.^[127] A great success was achieved in 2010 with a solar cell based on the copolymer PTB7, based on the combination between a fluorinated TT unit and an alkoxy-substituted BDT. As a result, the PTB7:PC₇₁BM-based OSCs exhibited a record PCE of 7.4%. PTB7 was further optimized by side chain tuning; indeed, by replacing alkoxy side chains on the BDT unit with thienyl-based side chains, the analogous PTB7-Th polymer (also known as PCE10) was prepared.

Substantial improvements on PTB-based polymers were subsequently made through interfacial layer engineering. In particular, the use of a conjugated polyelectrolyte as a solution-processed buffer layer (on the top of the BHJ blend) in an inverted device structure led to the PCE improvements from 7.4% to 9.2% for PTB7-based cells^[128] and to 10% for those based on PTB7-Th (or PCE10):PC₇₁BM.^[129]

Isoidigo (II) Units: Another family of low bandgap polymer is based on the isoidigo unit.^[130] II is a strong electron-withdrawing building block due to the presence of two adjacent and conjugated lactam rings also creating intramolecular interactions able to planarize the structure, thus favoring interchain π - π stacking. Isoidigo-based materials, first reported by Reynolds and co-workers,^[131] have quickly become popular for organic electronics because of their ease of synthesis. In 2011 Wang et al. reported a new low bandgap polymer (poly(N,N'-bis(2-hexyldecyl)isoidigo-6,6'-diyl-alt-thiophene-2,5-diyl)-1) with alternating thiophene and isoidigo units. A PCE of 3.0% and a high open-circuit voltage of 0.89 V were realized in polymer solar cells, which demonstrated the potential of this class of polymers. Later, they also reported a series of copolymers based on the combination of II and quinoxaline (Qx) units.^[132] By a fine-tuning of the molecular structure, it was possible to prepare BHJ devices with PCEs of >6% and a V_{OC} of 0.93 V.^[133] Two novel conjugated polymers based on BDT and isoidigo units linked with a TT unit as a π -bridge were designed and synthesized, yielding PCE up to 8% when implemented in BHJ solar cells.^[134]

Best performing Materials: Benzodithiophenedione (BDD)-Based Units: A nonclassical electron-withdrawing unit, benzo[1,2-*c*:4,5-*c'*]dithiophene-4,8-dione,^[135] has recently emerged in the field of organic PVs due to its peculiarities, such as planar molecular structure, low-lying HOMO level, several substitution sites for functionalization, and a good self-assembly capability. Compared with the device performance evolution of other donors, BDD-based polymer showed a rapid progress in few years, passing from the first PCE of 4.5% reported for in 2012 up to 16% in 2019^[136] and 17% in 2020.^[137] Remarkably, this rapid evolution in terms of PCEs is concomitant with the parallel development of the NFAs that have been combined with BDD-based polymers to reach the last impressive results.

In parallel, a promising series of wide bandgap copolymers based on fused-ring acceptor units were prepared by Ding and co-workers.^[138,139] These fused building blocks have strong electron-withdrawing character and extended molecular planes, affording systems with improved π - π stacking, charge mobilities, and low-lying HOMO levels, likely enhancing V_{OC} , J_{SC} , and FF of the corresponding BHJ cells. As a result, the polymer D16 (Figure 5), based on a fused-ring thiolactone unit (5H-dithieno[3,2-*b*:2',3'-*d*]thiopyran-5-one), delivered a PCE of 16.72% when blended with Y6 as an acceptor material.^[140] Recently, a more efficient copolymer donor D18 (Figure 5) using a modified fused-ring unit (dithienobenzothiadiazole [DTBT]) was reported.^[33] The D18:Y6-based solar cell showed an impressive PCE of 18.22% (certified 17.6%), which is actually the highest efficiency reported for OSCs.

Electron-Acceptor Materials: Since 1995, fullerene derivatives (in particular, the soluble PCBM) have been the most used and studied acceptors in OSCs.^[141] They provide optimal

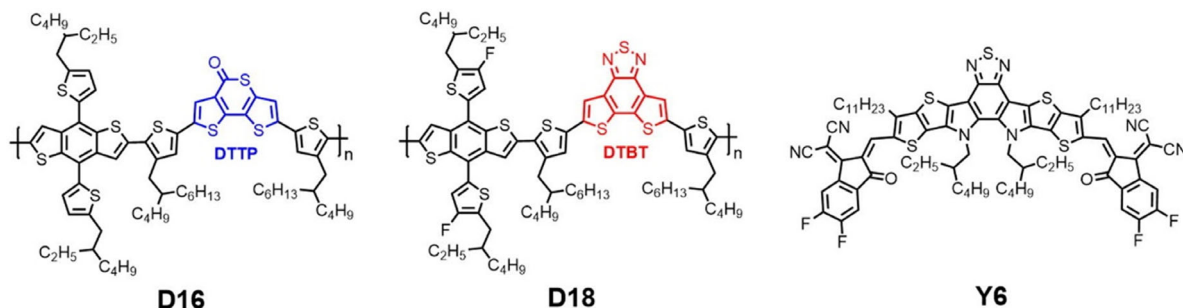


Figure 5. Chemical structures of D16, D18 (donors), and Y6 (NFA). Reproduced with permission.^[33] Copyright 2020, Elsevier.

isotropic electron-transporting properties and nanoscale morphologies of the BHJ blend due to the good miscibility with almost all donor polymers.^[142] However, despite these advantages, fullerenes exhibit significant limitations, such as poor light-absorption properties, limited energy-level tunability, and morphological and/or photochemical instability of corresponding BHJ blends.^[40,143]

To further push up the performance of OSCs, tremendous efforts have been directed to overcome these limitations, introducing new class of acceptor materials (polymers and small molecules) defined as NFAs.

At the beginning, NFA-OSCs showed limited success in achieving similar PCEs to fullerene-based devices. However, recent breakthroughs and results quickly revitalized NFA-OSCs, in particular, with the development of small molecular acceptors (SMAs).^[144,145]

Among NFAs, perylenediimides (PDI) have been one of the first class of materials widely used and investigated in BHJ solar cells because of their good electron mobilities and propensity to self-organization.^[146,147] Through fine structural modifications/functionalizations and optimized processing conditions, PDI-based OSCs led to PCEs up to 11%.^[148] In parallel, new classes of acceptors with alternative molecular structures were designed and tested. It was found that the molecular structures containing electron-donating (D) and electron-accepting (A) fused rings as building blocks (analogously to the strategy used for donor polymers) were particularly efficient in BHJ devices. For instance, the A–D–A architecture was adopted to design 3,9-bis(2-methylene-(3-(1,1-dicyanomethylene)-indanone))-5,5,11,11-tetrakis(4-hexylphenyl)-dithieno[2,3-d:2',3'-d']-s-indaceno[1,2-b:5,6-b']dithiophene and 2,2'-(2Z,2'Z)-((4,4,9,9-tetrahexyl-4,9-dihydro-s-indaceno[1,2-b:5,6-b']dithiophene-2,7-diyl)bis(methanylylidene))bis(3-oxo-2,3-dihydro-1Hindene-2,1-diylidene)dimalononitrile derivatives, which have strong visible–near-infrared (NIR) light-harvesting capability and good electron mobility, delivering higher J_{SC} and PCEs than those of fullerene-based OSCs.^[149] To further improve light harvesting (lower bandgap), Ding and co-workers^[150] developed stronger A–D–A NFAs using more electron-donating (CO-bridged) fused rings, which through a proper device and processing conditions optimization led to the device efficiencies greater than 14% (ternary solar cell).^[151]

The great potential of low bandgap NFAs was confirmed by Yuan et al.,^[152] who prepared a highly efficient low bandgap acceptor, Y6 (A-DAD-A structure), which is actually one of the

best performing NFAs in OSCs (PCE up to 18% in combination with donor D18, Figure 5).

3.1.2. Perovskite Photoactive Materials

Due to its low cost and abundant raw material elements, perovskite materials are considered to be one of the new generation of PV power generation active materials with great development potential. The generalized perovskite material refers to the material with the simple structure of ABX_3 , and its basic structure is shown in **Figure 6**. The B-site atom coordinates with the adjacent six X atoms to form a BX_6 octahedron, which is extended in a 3D frame structure; A-site atoms occupy the gap formed by the octahedral common vertices and form an AX_{12} dodecahedron with the nearest X atoms.^[153] In 2009, Miyasaka and co-workers applied $CH_3NH_3PbX_3$ ($X = Br$ or I) to dye-sensitized solar cells for the first time and achieved a photoelectric conversion efficiency of 3.8%.^[154] After more than ten years of development, the certification efficiency of PSCs has reached 25.2%, which is comparable to traditional polysilicon and thin-film solar cells.^[155] An obvious feature of perovskite is the adjustable composition in its A, B, and X sites. Each site can contain single or mixed ions, as long as the size of the ions meets the Goldschmidt tolerance factor.^[156] The combination of various perovskite

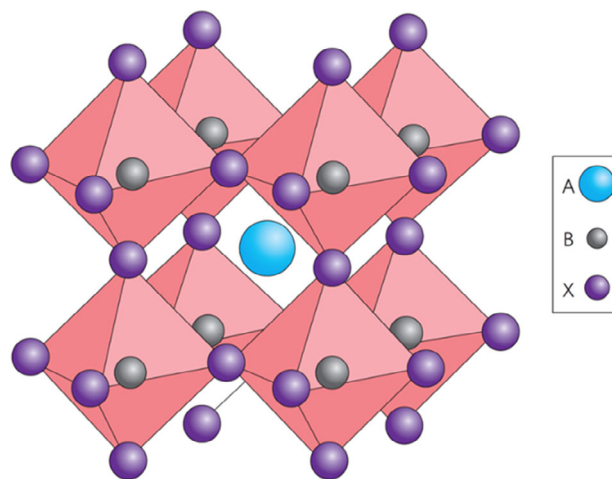


Figure 6. Crystal structure of ABX_3 . Reproduced with permission.^[292] Copyright 2015, Springer Nature.

components corresponds to perovskite materials with different photoelectric properties. Researchers have conducted a lot of research to adjust the perovskite components to improve the efficiency and stability of the PSCs.

Methylammonium-based perovskite MAPbI₃ is the first hybrid perovskite compound investigated as an efficient active layer in this class of solar cells, and still most of the investigations appearing in the scientific literature focus on this material. The high conversion efficiencies reached using MAPbI₃ are negatively balanced by the presence of a heavy metal such as Pb and especially by the poor stability of the system with respect to temperature, humidity, and UV light exposure. The main research efforts in selecting suitable active materials are devoted to finding stable variants of single hybrid perovskite (substitution of the organic cation (A-site) with other organic molecules and/or inorganic cations; partial substitution of iodine (X-site) with other halide anions).

The A-site ion mainly plays a role of lattice charge compensation. The size of the A-site ion will cause the expansion or contraction of the crystal lattice, which will affect the bond length of metal ions and halogen ions, and then affect the bandgap of the material.^[157,158] Substitution of MA (ionic radius: 2.70 Å) with a slightly larger cation such as HC(NH₂)₂ (FA, ionic radius: 2.79 Å) without altering the crystalline structure has shown a better stability of perovskites.^[159] Compared with MAPbI₃ (1.55 eV), the bandgap of FAPbI₃ (1.48 eV) is more suitable, which allows greater potential in delivering higher PCEs.^[159] However, the photoactive black phase (α -phase) of FAPbI₃ is thermodynamically unstable at room temperature. An FA MA mixed perovskite system (FAMA) with a more stable α -phase becomes an excellent alternative in high performance and more stable PSCs.^[160,161] Moreover, Cs has a smaller ionic radius (1.81 Å) than MA and FA, which serves as the effective “phase stabilizer” of the α -phase of FA-based perovskites.^[51] In 2016, based on the widely used FAMA system MA_{0.17}FA_{0.83}Pb(I_{0.83}Br_{0.17})₃, the effect of incorporation in A-site was systematically investigated by Saliba et al.^[162]

In recent years, inorganic PSCs have attracted more and more attention due to superior thermal stability and photoelectric performance.^[163] In 2012, inorganic PSCs based on CsSnI₃ were reported for the first time, with an efficiency of 0.88%,^[164] and the PCEs based on CsSnI₃ increased to 2.02% in 2014.^[165] Later, more stable CsPbX₃ materials were applied to inorganic PSCs, and its efficiency has exceeded 11% in a short period of time.^[166,167] At present, most inorganic perovskites still use Pb-based perovskites, in which the I atom at the X position can be replaced by Br, depending on the number of replacements by Br. The highest reported inorganic PSC is based on the β -CsPbI₃ light-absorbing material system; using phenyltrimethylammonium chloride (PTACl) to passivate the surface of the perovskite, the PCE of the device reached 19.03%.^[168] Studies have shown that CsPbI₃ and CsPbBr₃ can maintain a stable structure and composition at 460 °C close to their melting point.^[169]

On the other hand, the bandgap value of single-component halogen substitution is not less than 1.5 eV, and halogens Cl, Br, and I are used as the substituent groups of X-site to control the energy bandgap of perovskite.^[170] Using PbCl₂ to replace PbI₂ in the precursor solution [n (MAI):n (PbCl₂) = 3:1] can improve PCEs. Noh et al. prepared CH₃NH₃PbI_{3-x}Br_x light-absorbing layer with different ratios of Br/I with good humidity

stability, and the best PCE was 12.3%.^[157] Zhou et al. increased the PCE of the CH₃NH₃PbI_{3-x}Cl_x light-absorbing layer to 19.3% by optimizing the interface and annealing process.^[171]

The environmental sustainability of perovskite is addressed following mainly two directions: 1) finding high efficient recycling processes of lead-based compounds (it has been shown that 99.7% of Pb can be safely recycled^[172]) and 2) substituting the heavy metal (B-site) with nonpollutant elements, such as Sn and Bi, in the structures. With respect to lead-free perovskites, the most promising results, to date, have been obtained, working on all inorganic double perovskites with the formula A₂B(I)B(III)X₆, where A is an alkali metal (Na, K, Rb, and Cs), B(I) is a monovalent (Cu, Ag, and Au), B(III) is a trivalent metal (Bi, Sb, and In), and X is a halide anion (F, Cl, Br, and I).^[173–176]

3.2. Functional Materials

3.2.1. Interlayers

In a typical solar cell, the photoactive blend is sandwiched between two electrodes (cathode and anode) that allow an efficient extraction of photogenerated charges. More in detail, the structure also includes functional layers at the active layer/electrode interfaces able to optimize the charge collection process at the electrodes.^[177] Indeed, although the internal electric field within a solar cell drives the flow of charges anisotropically toward the correspondent electrode, field-independent diffusion processes can occur, and free charges in proximity of the opposite electrode can recombine at the interface resulting in performance losses for the device.

These additional ILs, commonly defined as HTLs or ETLs, play a crucial role in terms of performance and stability both for OSCs^[178] and PSCs.^[179] There are many similarities in the kind of ILs that are used for both technologies. In addition, in some cases, ILs have the additional role of “optical spacers,” enabling the modification of the light distribution inside the solar cell stack, resulting in an improved active layer absorption and, hence, enhanced solar cell performance.^[180,181]

An optimal IL should be able to simultaneously satisfy several requirements, such as: 1) an ohmic optimal energy level matches with the HOMO energy level of the donor (for HTLs) and the LUMO level of the acceptor (for ETLs); 2) high charge selectivity, promoting the charge extraction of majority charge carriers at the respective electrodes, thus avoiding charge accumulation and suppressing the extraction of minority charge carriers (e.g., HTLs (ETLs) select positive (negative) carriers, blocking negative (positive) carriers); 3) sufficient conductivity to avoid resistive losses; 4) optimal transparency to limit optical losses; 5) excellent morphological properties to enhance the interfacial quality with adjacent layers, thus avoiding the formation of defects, shunt pathways, and/or trap states; 6) ability to be easily processed (e.g., from solution), possibly at low temperatures and under environmental conditions; and 7) stable under working conditions/device operation.

Despite the difficulty to simultaneously fulfill all these requirements, different classes of materials (ETLs and HTLs) have been largely investigated, including: conducting polymers, metal oxides, crosslinkable materials, conjugated polymer electrolytes, self-assembled functional molecules, and graphene-based

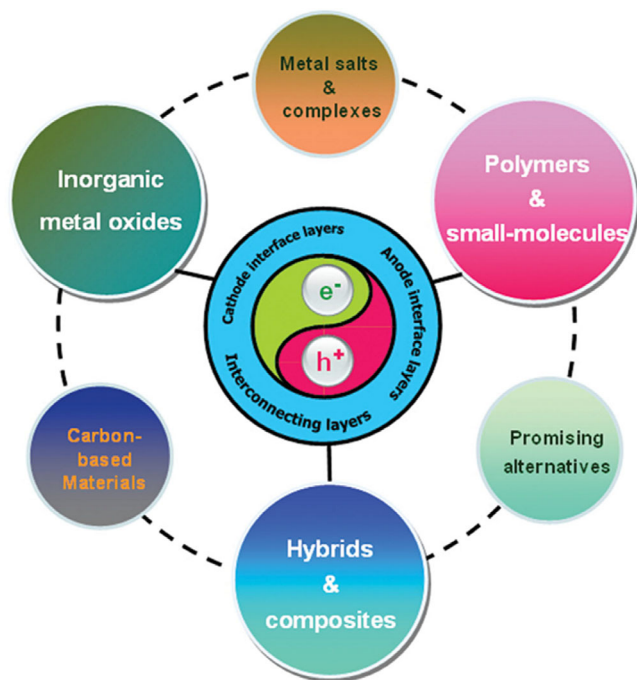


Figure 7. Schematic illustration of material categories for cathode interface layers (or ETLs), anode interface layers (or HTLs), and ICLs commonly used in OSCs and PSCs. Reproduced with permission.^[178] Copyright 2016, Wiley-VCH.

materials (Figure 7), thoroughly discussed in several dedicated review articles.^[177,178]

Among ETLs, n-type metal oxides (e.g., ZnO, TiO_x, and SnO_x)^[182] and their doped derivatives,^[183] having deep-lying energy levels, are predominant and well-consolidated ILs for the fabrication of standard and inverted PSCs, because of their optimal solution processability, intrinsic and environmental stability, optical transparency, and excellent capability to extract/transport electrons. In addition, to improve the compatibility of ILs with organic/hybrid blends, solution-processable organic materials (small molecule and polymers) have been recently used as interface materials for efficient solar cells.^[184,185] Moreover, as already mentioned, the possibility to modify the chemical structure of organic molecules offers the great advantage to finely tune all key properties, such as optical/electronic behavior, energy levels, and also the dipole orientation of self-assembled monolayers lowering the WF of cathodes/anodes and increasing the built-in potential of OSCs.^[186]

While ETLs have low WFs for electron collection, the HTLs should have high WFs to match the HOMO levels of the donor to facilitate hole extraction. To date, many hole-transporting materials, such as organic conductive polymers, metal oxides/sulfides, graphene oxides, their hybrids/composites, and other alternatives, have been designed for both conventional and inverted OSCs.^[178]

Among them, the conducting polymer poly(3,4-ethylenedioxythiophene) polystyrene sulfonate (PEDOT:PSS) is one of the most used and investigated HTLs due to its excellent processability and electronic/electrical properties, even though its acidity and hygroscopic nature, combined with a phase-

segregation tendency, can significantly influence the stability of the resulting devices.^[187] Vacuum-processed p-type metal oxides are also extensively used, offering optimal results both in terms of device performance and stability. However, they are not fully compatible with wet large-scale manufacturing processes. Therefore, analogous solution-processable metal oxides, such as MoO_x, VO_x, NiO_x, and WO_x, which combine optimal processability, environmental stability, and satisfactory device performance/lifetime, have been successfully demonstrated even though there are still open challenging tasks.^[188,189]

Analogously to OSCs, ILs also play a crucial role for the development of PSCs.^[179]

The choice of ETLs, also acting as hole blocking layers, strongly depends on the architecture of PSCs. In n-i-p geometry, the selection of the material does not depend on the solvent used in wet deposition or on the annealing temperature (in case of FTO film on glass, the annealing temperature can be of the order of 500 °C). The latter condition is not valid in the case of flexible photocathodes because of the limited annealing temperature compatible with the plastic supports. Metal oxide semiconductors (TiO₂, ZnO, SnO₂,...) are the most commonly used materials,^[190] but also organic semiconductors, as in the case of OPV, are also used. TiO₂ is commonly used in this kind of cells despite it shows UV instability and needs relatively high annealing temperatures with respect to other oxides such as SnO₂.^[191] In inverse geometries, the ETL deposition occurs on top of the perovskite layer, limiting both the annealing temperature and the nature of the solvent that need not to decompose or dissolve the active layer. In this configuration, the most common used materials are organic fullerenes or nonfullerene compounds.

Concerning HTLs, doped spiro-OMeTAD is the most used p-type material in PSCs because of a very good matching between the valence band of perovskites and the HOMO level of the molecule, giving rise to a high open circuit voltage V_{OC}. The instability induced by the doping of spiro-OMeTAD and the relatively high cost of the materials have shifted the focus of researchers to other organic HTLs, such as PEDOT:PSS, P3HT, and graphene oxide, and to inorganic materials, such as CuI, CuSCN, and NiO.^[192]

Another strategy relies on inverted PSCs based on fully organic HTLs. Among these alternative interfacial materials, organic ILs exhibit unique characteristics, including flexible, low-temperature solution processability, and good electrical and structural property tunability. Therefore, they show an immense potential to propel PSCs toward future advancements. In virtue of their tunable energy band structure, controllable interfacial wettability, tunable carrier mobility, and permanent interface dipole action, the solution-processed organic ILs play various roles in both regular and inverted PSCs.

Clearly, the considerations related to photoactive materials in the scale-up of solar cell technologies also apply to other functional materials and ILs. Technological advancements for real setting applications require a wide range of materials properties to be finely tuned to improve overall conversion efficiencies and, at the same time, to allow the development of fabrication processes and application cases at large scale.

As mentioned before, considerations about ease of fabrication, stability, availability of raw materials, cost, and environmental impact play a significant role for the development of materials

for ILs in the industrial context. In this respect, organic small molecules and polymers, beside the chemico-physical properties mentioned earlier, also offer a great potential as ILs, in the context of both OSC and PSC technologies.

Recent work has also highlighted the possibility of using organic molecules as ILs for the large-scale development of PSC technologies. The molecular engineering of organic small molecules as ILs for the scale-up of PV technologies is currently a very active field of research, especially with regard to the development of HTLs for PSCs, which is one of the most crucial aspects of the whole technology.^[193–196] In particular, the use of a new, low-cost, dopant-free HTL in mixed-ion solution-processed PSCs allowed to achieve the record PCE of 19.7%.^[85] This result was obtained through an approach based on the integration among rational molecular design, device fabrication, and characterization, which shed light on the nanostructure and molecular aggregation of the HTL. This work led to the identification of copper (II) phthalocyanines (CuPcs) derivatives substituted with arylamines, reaching the highest PCE ever reported for PSCs using dopant-free HTLs. Long-term stability of the PSC was also achieved, due to the inherent thermal and chemical properties of the dopant-free CuPc. The approach proposed also highlights the link between the molecular structure of ILs and the properties of devices, showing a route for the engineering of dopant-free HTLs to be used in the manufacture of low-cost and high-performance PSCs. The integrated approach based on rational design and computational modeling proved to be central in identifying and anticipating the synthesis of new materials with specific structural functions in complex devices. These studies also suggest the need for a wide tool of modeling and experimental techniques for the rational design of novel materials for ILs in PVs.

3.2.2. Charge Extracting Electrodes

The choice of materials for manufacturing the electrodes of PV solar cells is also crucial from the point of view of both basic functioning phenomena and aspects related to large-scale production.^[197,198] One of the basic requirements of materials for solar cell electrodes is a favorable alignment of their electron energy levels with respect to those of the ILs/active materials. The cathode and anode materials should be able to extract electrons and holes, respectively, from the device with an ideally minimal energy barrier. The magnitude of this barrier depends on complex interface phenomena and can be approximated to the difference between the WF of the electrodes and the energy level of the active materials only in very particular cases (Schottky–Mott limit). In most cases, however, the efficiency of the coupling between the active layers and the electrodes is related to the peculiar chemico-physical properties of the materials involved, which can lead to a strong renormalization of the electron density distribution across the interface.

Relatively few materials couple an excellent intrinsic conductivity (required for external electrical outcoupling) with favorable energy level alignment at the interface with the active system. In addition, at least one of the electrodes must display a sufficient level of optical transparency.

Materials commonly used as electrodes, which fulfill these minimal requirements, are pure metals or conducting metal

oxides. In recent years, several research efforts have been targeted to the development and optimization of TCOs to be used in solar cells. The most common TCO used in solar cell applications is undoubtedly ITO, also doped with other elements. ITO can couple remarkable electrical conductivity with good optical transparency and is ubiquitously used as a transparent electrode in organic and hybrid electronics applications. Significant research efforts, however, have demonstrated the possibility of using other systems, including organic conducting and doped polymers, nanostructured carbon materials, or nanocomposites, as efficient electrodes for PV solar cells. The use of noncrystalline materials can also significantly improve the mechanical properties of novel PV systems, for example, in terms of flexibility and conformability.

Nevertheless, other significant elements of the electrode fabrication technology greatly impact on the development of solar cells. One of the aspects that must be considered concerns the cost of raw materials and related to fabrication processes. Among the various (relatively) expensive components, including carrier-transport layers and encapsulation materials, electrodes (transparent conductive substrates and/or high-priced metals such as Au) usually represent another significant fraction of the whole cost for the fabrication of solar cells.^[163] The economic advantages stemming from the use of low-cost materials and processing for the fabrication of the active layers in organic and hybrid solar cells can, therefore, be undermined by the cost needed for the fabrication of electrodes.^[199]

Pure noble metals, such as gold, constitute an intrinsically limited (and expensive) resource. Moreover, current methods allow the reliable fabrication of metallic electrodes by high-vacuum thermal processes, with a great impact on overall fabrication costs and limiting the scale-up potential of the technology.^[200]

Similar considerations apply to electrodes based on TCOs, usually fabricated by low throughput and relatively inefficient vacuum deposition processes. The use of wet processes, in contrast, is considered as a low-cost and potentially scalable alternative for the fabrication of electrodes.

The application of additive, solution-based, large-area deposition technologies is indeed key to the development of new solar cell systems. Solution-based processes are compatible with most organic materials, but can also be used to fabricate metallic electrodes through dispersion of metallic or metal-oxide nanostructures.^[201,202] In contrast to metals and metal oxides, organic and carbon-based materials constitute a low-cost alternative for the fabrication of electrodes.^[203,204] Recent research work has demonstrated the potential of low-dimensional carbon nanostructures, such as graphene, carbon nanotubes, or composites, to realize highly conductive and transparent electrodes for solar cells.^[205,206]

Nevertheless, wet processes can unleash their full potential in the fabrication of electrodes based on organic molecular or polymer materials. The relatively low conductivity of organic materials is usually alleviated by doping the electrode, a process that, however, can limit the stability of the device.

Therefore, the realization of electrodes for next-generation solar cells must fulfill a broad set of requirements, constituting a crucial step in the engineering of new PVs technologies. These requirements can be summarized as follows: 1) suitable energy levels and possibility of tuning the electrode levels to match those

of the active systems, through formation of an efficient interface with large charge injection/collection ratios; 2) high conductivity of the electrode materials: metal and metal oxides exhibit excellent intrinsic conductivities with respect to molecular and organic systems, and low-dimensional carbon nanostructures are a metal-free alternative; 3) good optical transparency: organic materials with low optical absorption can be synthesized and processed quite easily, whereas metals or metal oxides may require special patterning techniques to achieve the required optical transmittance; 4) low fabrication cost, including raw material and processing costs, and ease of processing, including large-area, high-throughput contexts; and 5) long-term chemical and structural stability.

The selection of the proper materials and fabrication techniques for the realization of electrodes is, therefore, one of the critical variables for the optimization of solar cell technologies.

3.3. Multiscale Approach to Materials Design

The intrinsic properties of materials used in PV solar cells are deeply related to the overall efficiency and devices. In recent years, theoretical frameworks have been developed for correlating materials properties and device architecture to the optoelectronic properties of PV systems and extended to the case of OPV and PSC technologies.^[207] Theoretical methods for the modeling of solar cells rely, in most cases, on the application of detailed balance to solar cells.^[208] These phenomenological approaches allow the prediction of PCEs of solar cells as a function of empirical parameters, derived either from experimental data or from parameter fitting.^[209] For example, an ideal efficiency of $\approx 20\%$ has been predicted for single-layer OSCs with NFAs as a function of phenomenological device parameters (**Figure 8**).^[210]

However, the complexity of the relationship between the structure of matter at the atomistic/molecular level and properties and behavior in devices hinders a direct approach to the design and engineering of materials for PVs. This issue requires, therefore, the development of a rational, predictive framework connecting the properties of materials across different scales.

Recent developments in multiscale modeling methods have enabled the application of predictive simulation tools to the

design and engineering of new materials for applications in electronics and optoelectronics.^[211–213] In several application scenarios, including PVs, multiscale modeling is used to unravel the complex relationship between the structure of basic components and properties occurring in active materials in a realistic working environment.^[214–216] In general, multiscale approaches consist in defining models and, consequently, descriptors of the properties of materials and chemically physical phenomena across a wide range of spatial and temporal scales.^[217] The multiscale approach to investigation of matter is particularly relevant for molecular and nanoscale materials, where the properties at the microscopic scale impact on the working mechanism of complex, multifunctional devices.^[218,219] Traditional multiscale modeling techniques rely on analytical formalisms for connecting models describing the properties of a system at different scales.^[220] However, this approach has a quite limited use in several practical cases, due to the intrinsically complex nature of technological materials. Conversely, approaches based on the development of specific and interlinked models for each physical scale of interest have recently gained much interest in the simulation of the properties of multifunctional materials.^[221,222] A typical example of this approach concerns the simulation of charge transport properties in organic semiconductors.^[223–225] Multiscale approaches based on model linking can transfer information on complex systems from a scale domain to neighboring domains.^[226,227] In the case of charge transport, microscopic models of intermolecular electronic coupling can be linked to mesoscale models of charge transport and, in turn, to continuum models of electrical currents in materials. From the technical point of view, this workflow implies performing simulations at different theoretical levels. For example, the results of density functional theory (DFT) calculations of electronic coupling can be used in upper-level simulations of charge percolation in molecular aggregates using kinetic Monte Carlo (KMC) approaches.^[228,229] These models can then be used to provide parameters for drift–diffusion models of full-scale devices. A phenomenological link among models at different scales can provide information on the interplay between details of the structure at the atomistic/molecular scale and the overall performance of devices. The development of a multiscale computational framework, tailored to a specific application,

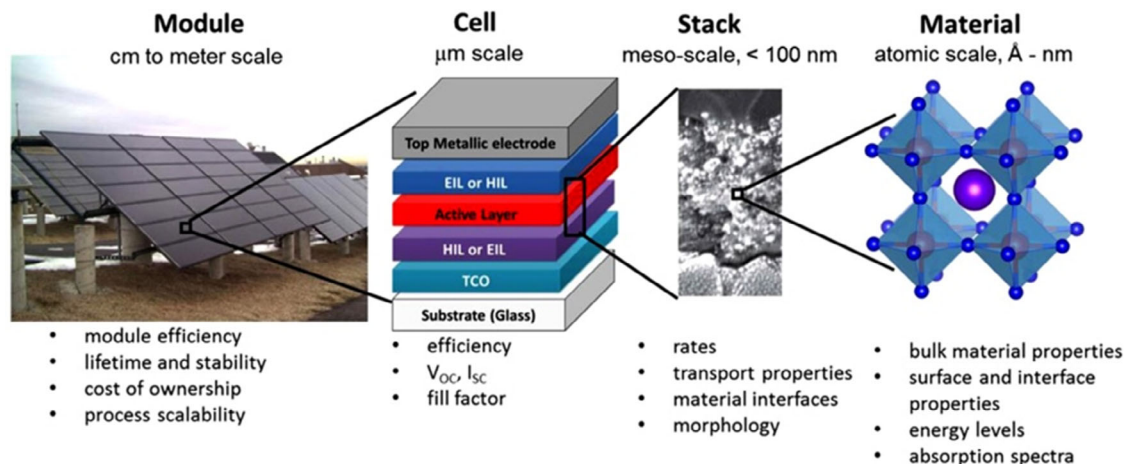


Figure 8. Scheme of the multiscale modeling approach to materials design. Reproduced with permission.^[293] Copyright 2018, Springer.

can enable the predictive evaluation of the potential performance of materials in devices, to be used, for example, in the screening of materials among a set of candidates or in the optimization of materials components and structural units.

Clearly, the efficiency of the whole computational workflow is related to the numerical performance of the simulation methods applied to the chemophysical models and to the strategy applied to enable the multiscale linking. In this respect, the application of large-scale and high-performance computing (HPC) infrastructures is a crucial step in the implementation of efficient computational strategies.^[230] The application of fully in silico technologies for the development of new materials can, therefore, result in potentially fast, accurate, and low-cost alternatives to the experimental trial-and-error development of materials. In addition, the high throughput of data generated by state-of-the-art hardware and software infrastructures for numerical simulations has recently enabled the application of machine learning (ML) technologies to materials modeling, increasing the scope and predictive power of computational approaches.^[231,232]

As a result of the encouraging perspectives in several research fields, multiscale simulation approaches have recently been applied with success to the development of active and functional materials and interfaces for PVs applications. Quantum chemical methods, such as DFT, have been widely applied to predict the electronic and optical properties of materials for PVs, including small molecules, polymers, or inorganic systems.^[233,234] The level of detail offered by DFT calculations can, in principle, enable the definition of the relationships between structural details of materials and resulting properties, thus allowing a fine-tuning of the chemical structure and composition of materials with respect to a specific target.^[235,236] In comparison with simpler approximations, such as semiempirical calculations, or more accurate and much more expensive methods (coupled-cluster calculations, GW approach, etc.), the use of DFT often represents an optimal compromise between accuracy and computational load. Interestingly, time-dependent DFT calculations can predict, with high accuracy, the excited state properties of materials for PVs, thus providing detailed information on crucial quantities related to photoexcitation and exciton formation.^[237] The limited size of DFT models narrows the scope of electronic structure calculations to investigations on the basic properties of materials. In a multiscale perspective, the detailed information about the electronic structure of active materials needs to be coupled with higher-rank models describing, for example, nanoscale aggregation morphologies, dynamics, formation of interfaces, and several other phenomena occurring at different (higher) scales.

The transport of charge in materials for PVs can be simulated by coupling electronic structure properties to materials morphology at the nano- and mesoscale. The multiscale approach based on the integration between electronic- and mesoscale calculations has been widely used to evaluate the charge transport properties of materials for PVs. Computational methods have been used, for example, to predict the mobility of charges and excitons in photoactive materials, such as donor/acceptor pairs in OPVs or halide perovskites. Similar methods have also been applied to other materials of interest in PVs applications, such as charge transport layers and interfaces.^[238] This approach demonstrates

the potential of linking models across different scales to predict materials properties for technological applications and highlights the crucial role of accurate theoretical methods in assessing the morphology and structure of matter at the nanoscale.

Most relevant phenomena related to the generation and transport of charge are, however, intertwined with nanoscale aggregation mechanisms.^[239] Therefore, the development of reliable models for the simulation of the structural properties and dynamics of macromolecular, supramolecular, nanoscale aggregates, and nanoclusters of materials for PVs has become a crucial ingredient for the realization of predictive modeling platforms.^[240] Simulation methods generally referred to as molecular mechanics allow to simulate the time evolution of the system under investigation (molecular dynamics), providing information about the dynamical properties of materials. At a larger scale, further approximations can be made, and the system can be described at a coarser level of detail, that is, in terms of particles including a variable set of atoms (up to a few tens), thus greatly reducing the computational load. This set of methods referred to as coarse-graining (CG) enables investigations on model systems up to several micrometers in size and has been applied with success to the study of materials for PVs. The typical scope of simulation methods based on molecular mechanics is also compatible with detailed investigations of structural reorganizations at interfaces in materials for PVs.

Electronic, atomistic, and coarse-grained models can also be integrated with other particle-based methods to predict functional properties of materials for PVs. One of the most relevant applications of this approach is the integration among DFT, molecular dynamics/CG, and KMC methods for the multiscale evaluation of the electrical properties of materials and devices. More efficient methods for the simulation of materials, interfaces, and devices at the laboratory scale rely on continuum models. Here, the particle-based description is lost and is replaced by a description of the properties of the systems in terms of phenomenological parameters. The relatively simple formalism offered by continuum models allows the simulation of most of the macroscopic properties of PVs solar cells at the full device scale and the prediction of basic quantities, such as currents, potentials, PCE, light outcoupling, etc., in terms of simple materials properties and geometries.^[241–243] The relationship between materials and device parameters and performances allows the prediction of maximum theoretically achievable efficiencies of solar cells in realistic conditions: 1D simulations predict a PCE exceeding 25% for OPV tandem cells and of about 30% for PSCs.^[244,245] In multiscale approaches, however, these parameters, as, for example, bulk properties of materials or interface properties, can be derived by lower-scale particle-based simulations. This approach allows a consistent integration between the properties of the basic constituents of PVs systems and resulting device properties. The possibility of simulating PVs systems at the full-device scale enables the fundamental linking between materials properties and experimental work. In addition, continuum models can potentially be extended to the simulation of macroscopic systems, such as large-scale modules or integrated devices. In this respect, a truly predictive multiscale approach to materials modeling can greatly accelerate the development of materials for PVs. Recent studies demonstrate that the integration between multiscale modeling approaches and

experiments can provide an efficient platform for the development of PV systems.^[246,247] The potential of modern computational infrastructures can indeed sustain a significant throughput of data that can parallel experimental work. The generation of a large amount of computational and experimental data can enable the application of data-driven approaches for the development of next-generation solar cells. These integrated, high-throughput approaches can assist the definition and identification of interconnected figures of merit that will be crucial in the scale-up of PV technologies.

4. Toward Real Setting Applications

Crystalline silicon is the first generation of solar PV technology that still dominates the market because of its long lifetime under operational conditions and best cost/performance balance. Crystalline silicon panels cover over 92% of the global PV market and generate nearly 3% of global electricity.^[248] Although single-crystal silicon solar cells provide higher PCE than multicrystal silicon solar cells, polycrystalline Si is the most widespread technology, because it offers the best ratio between initial cost and electricity production. To date, the polycrystalline Si large modules (>14 000 cm²) have a certified PCE of 20.4%.^[43] Due to the continuous improvements, power generated from solar PV is, to date, competitive with that of power plants based on fossil fuel,^[249] even though the environmental impact arising from the recycling and disposing of decommissioned silicon solar plants is still an open issue.^[250–252] To cut the cost of silicon PVs, thin-film solar cells were considered as an alternative candidate to replace the first-generation PV products. Nevertheless, their lower efficiency with respect to that of silicon allowed only a marginal PV market penetration (<10%),^[248] and toxic chemicals, such as Cd in prevailing thin-film CdTe-based solar cells, pose even more relevant environmental problems.^[252] All of these issues of the established first- and second-generation PV technology prompt the urgent development of a third generation of PV technologies.

4.1. Industrial Processing and Design

One of the distinguishing and enabling features of the third-generation PV technology is the industrial manufacturing process that increases the production yield and contributes to decrease the costs of the technology. At the laboratory scale, spin coating is the commonly used method for preparing OSCs and PSC thin films. However, this method is not entirely suitable for large-scale production, because it does not guarantee the required reliability at the needed production yield.^[252] For large-scale film deposition, the R2R method guarantees high throughput device manufacturing, leading to an increase in the product yield and to the reduction of production costs.^[250] The R2R method involves a long sheet to be used as a substrate, requiring a certain degree of mechanical flexibility that is, for example, guaranteed by polymeric materials, such as polyethylene terephthalate (PET), polyethylene (PE), polyethylene naphthalate (PEN), polypropylene (PP), polyimide (PI; commercial name: Kapton), or polyamide (PA; commercial name: Nylon).^[251] In the manufacturing process, the flexible sheet is first unwound from the roll and then

passed through the coating or printing box to deposit the ink pattern onto the sheet surface, and is then again rewound on another roll. Each layer of the OSC and PSC structures can be realized by coating and printing, by integrating, in the process, the steps of heating, drying, UV curing, etc. In 2014, Krebs and co-workers presented the first fully R2R-processed flexible polymer tandem solar cell modules with an active area of 52.2 cm².^[253]

“Coating” and “printing” are usually regarded as two methods that can meet the requirements of the R2R process.^[254] Schematic diagrams of these coating and printing technologies are shown in **Figure 9**. With the coating method, a layer of active material is formed on the substrate by knife/blade coating, slot-die coating, spray coating, or brush coating. With the printing method, the active layer is fabricated by inkjet printing, screen printing, gravure printing, flexographic printing, and pad printing.^[255] Among all these methods, slot-die coating and screen printing are reported as the most useful methods in the large area R2R processing of OSCs.^[255] In addition, the printing or coating methods used for the deposition of the back electrode not only require to form good contact with the photoactive material (e.g., BHJ or perovskite layer) but also should not physically and/or chemically damage the underlying layer/interface.^[256] In addition, the different layers should tolerate stress and strain actions occurring during bending of the devices; small crystalline grains perovskite films show larger resilience than large crystalline grains to bending processes, being more strongly bound to the substrate and with less tendency to break the single grains by introducing more grain boundaries.^[257]

It is worth mentioning that in R2R processing, a higher thickness tolerance of the active materials is required. Indeed, thin active layers are inappropriate to fabricate large-area OSC and PSC, because many point defects can originate in the active layer, which decreases the reliability of the process and the manufacturing yield.^[255] Wang et al. reported an OSC based on NT812: PC71BM with a 340 nm active layer thickness and a PCE of 10.33%, which decreases to 8.35% when the thickness reaches 1000 nm.^[255] Noteworthy, the use of thickness-tolerant materials is a crucial factor to take full advantage of the R2R fabrication.

Although the PCE of laboratory-scale solar cells have achieved a certified 17.6% for single-junction OSCs^[33] and a certified 25.2% for PSC,^[43] the realization of large-scale modules with high PCE is limited by the decrease in PCE with the increasing device area, due to the nonuniformity of device fabrication, structure defects, larger ohmic loss, and loss of active area from interconnection.^[34]

The design of the module is very critical to obtain efficient large-area modules. Indeed, a good modular design can minimize the electrical losses, the geometric FF (GFF) losses, and the optical losses.^[258] To date, the highest efficiency of OSC in submodules size sector (200–800 cm²) is 11.7% achieved by ZAE Bayern (Bavarian Centre for Applied Energy Research),^[43] whereas the PCE of PSCs small modules (800–6500 cm²) has reached 17.9% with an area of 800 cm².^[78] Clearly, there is still room for improvement, as the efficiency gap between small-area cell and large-area modules is still large. To achieve high performance and reproducible large modules, issues related to higher series resistance, lower shunt resistance, nonuniform films, dead areas, etc. should be addressed. These challenges involve a combined development of large-area

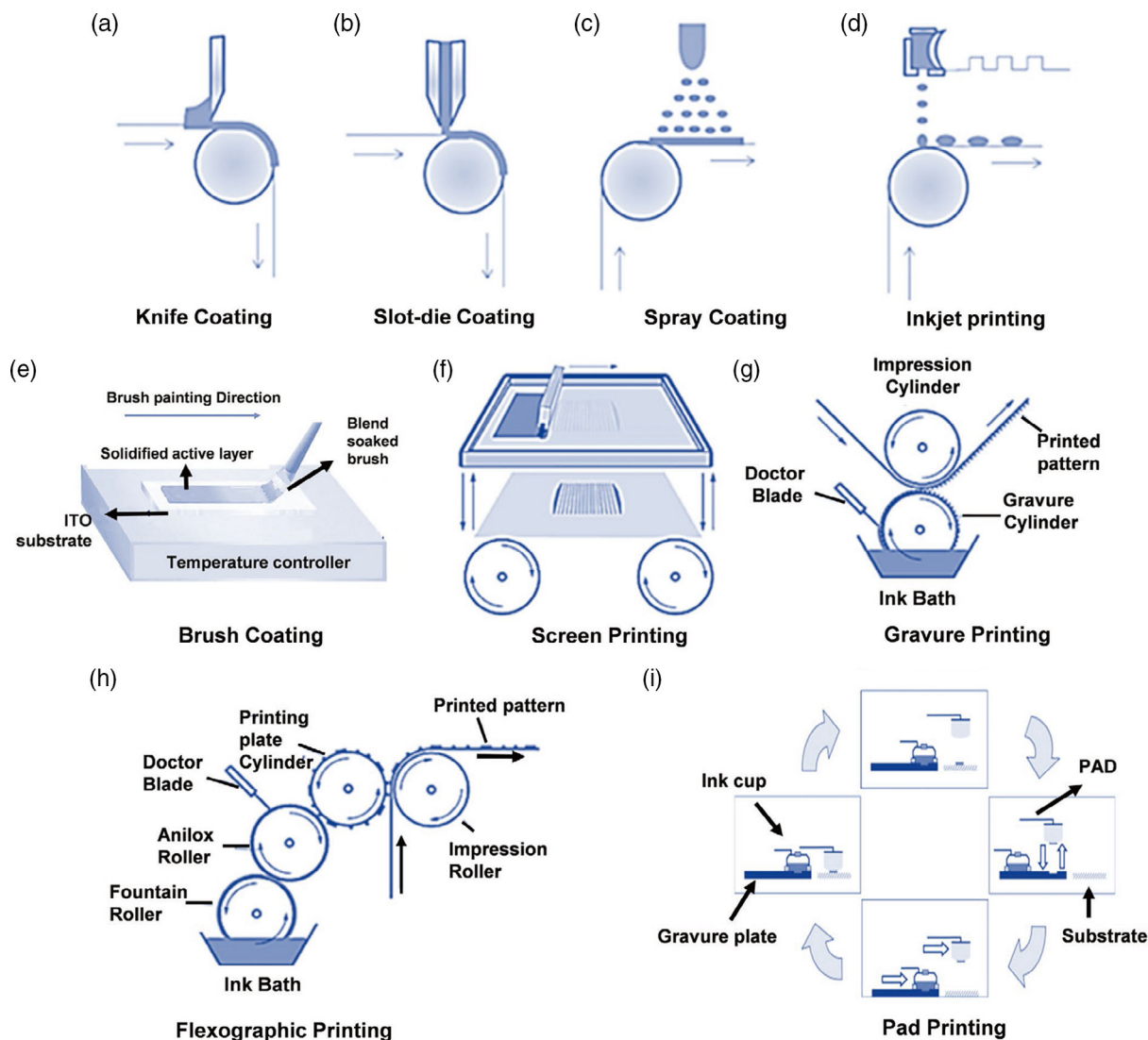


Figure 9. Schematic representations of a) knife coating, b) slot-die coating, c) spray coating, d) inkjet printing, e) brush coating, f) screen printing, g) gravure printing, h) flexographic printing, and i) pad printing. Reproduced with permission.^[255] Copyright 2018, Wiley-VCH.

deposition methods for the uniform coating of all device layers and the optimization of module design.

Durability is another important factor that can enable or prevent commercialization for a specific application. From the point of view of single cell, the factors that limit the cell stability during their whole lifecycles in terms of structural materials, including metastable morphology of active layers, diffusion of electrodes and buffer layers, effect of the external environment, including oxygen and moistures, irradiation, heating, and mechanical stress, have been clearly identified.^[40]

Despite the difficulty to define a specific metric to “quantify” the lifetime of modules under real conditions, some reports offer an interesting picture on the best and remarkable results in terms of device lifetime. For instance, Lidzey and co-workers^[259] reviewed the status of outdoor lifetime studies of OSCs, which represents the most complex and harsh scenario. Interestingly, the reported outdoor operational lifetime of certain organic

modules (mainly based on well-established and consolidated materials such as P3HT:PC₆₀BM) has now reached a period of several years; a promising result considering that less than ten years ago, typical device lifetimes were in the range of a few days to weeks. The reported results are also in perfect agreement with other studies, where the operational stability (outdoor conditions) of several organic-based modules (even commercial) was monitored, without significant losses, on the scale of months/years.^[34,260]

To go beyond the current state of the art in terms of stability and lifetime of modules under real operating conditions, encapsulation is a well-consolidated approach for the different types of solar cells. Interested readers can find more detailed information and results on dedicated review articles.^[261] Recently, Uddin et al. have comprehensively reviewed the encapsulation strategy for both PSCs and OSCs.^[262] Encapsulating devices with inorganic, organic, and inorganic–organic composite materials can effectively prevent the permeation of moisture and oxygen, thus allowing the

achievement of the desired reliability and device lifetime. The target water vapor transmission rate (WVTR) and oxygen transmission rate (OTR) for OSC and PSC are in the ranges of 10^{-3} – 10^{-6} g m⁻² day⁻¹ and 10^{-3} – 10^{-5} cm³ m⁻² day⁻¹ atm⁻¹, respectively.

Encapsulation materials should have a high dielectric breakdown matching the refractive index of other layers and high volume resistivity. They should be also dimensionally stable, low cost, and easy to process on complete devices, without damaging adjacent layers and/or components. Some recent studies also reported that the encapsulation layer could act as the UV light filters, particularly useful to hinder light degradation of organic components/layers within devices.^[263] In general, optimized and high quality encapsulation barriers/layers can greatly enhance the resulting device lifetime.

The complete encapsulation with glass is the simplest and best strategy to allow the achievement of targeted WVTR and OTR values. However, the main drawbacks of this strategy are: 1) incompatibility with flexible devices and 2) side permeation of oxygen and/or moisture, requiring the use of low-diffusivity edge seal materials.

The development of thin-film flexible encapsulation materials is of vital importance for the future application and commercialization of PSCs and OSCs. However, the presence of defects/local pinholes still represents a critical issue for achieving ultrahigh barriers encapsulation.

The use of organic and inorganic alternating multilayer thin films, in which the defects in the inorganic layers can be

passivated by the organic layer, offers a suitable solution to reduce intrinsic pinholes, thus allowing to achieve the best balance between gas barrier properties and flexibility.^[264]

4.2. Life Cycle Analysis (LCA)

During the last decades, the PV technologies have undergone a rapid and important expansion and evolution, now reaching a variety of solutions in the advanced research phase or already marketed. To define the energy and environmental impacts of these technologies, LCA studies related to these systems are constantly increasing, generating a broad literature with many results and analytical parameters ranging from the first generation (conventional silicon-based systems) up to emerging technologies.^[265,266] Recently, Blanco et al.^[267] investigated and reported the existing energy/environmental trends and hotspots through a systematic review and harmonization of LCA studies and results of the current state of the art and emerging PV. Despite the large uncertainties and variabilities in the reported LCA data and models, the harmonized results provide a general picture of the different PV technologies and their environmental impacts (with several impact categories), also highlighting potential hotspots for specific cases. **Figure 10** shows a radar plot with relative impacts of the different types of PV cells, where 100% corresponds to the impact score for a reference single-Si roof-mounted system.

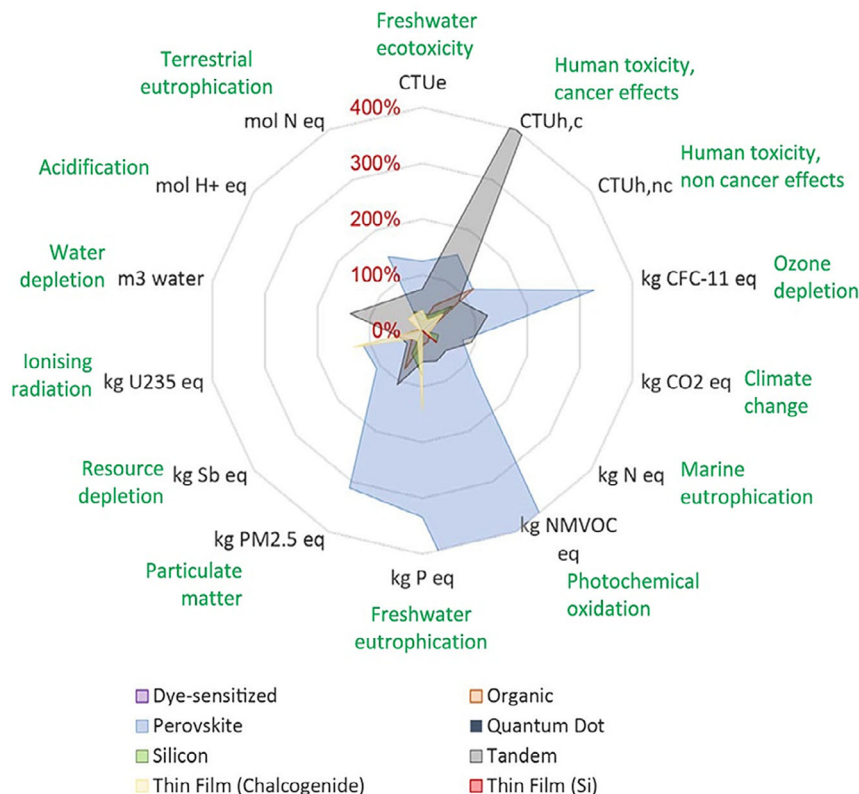


Figure 10. Relative impact scores for different PV technologies, compared with a reference single-Si roof-mounted PV system (100%). The plot is truncated at 400% for visualization purposes. Reproduced with permission.^[267] Copyright 2020, Wiley-VCH.

PSCs and tandem (inorganic/inorganic or inorganic/hybrid systems) cells exhibited a strong impact in several categories, exceeding the reference single-Si system by the factors of >2. Regarding PSCs, the potential hotspots are mainly related to active layer and ILs, which actually have the greatest impact on the pre-industrial module. This is due to the energy consumed during their preparation, annealing of the precursor solution, and used/residual solvents, rather than the Pb content. However, these aspects can be highly amenable to optimization.

From an overall environmental perspective, OSCs followed by thin-film silicon and chalcogenide exhibited several advantages, with an overall reduced footprint, compared with the reference system. It is worth noting that as many of the assessments are still based on early design concepts, in particular, for PSCs and OSCs, the reported results and considerations should not be used as arguments to hinder or discourage further research efforts on specific topics. Rather, they may be considered constructively to highlight and promote further research pathways that can result in more environmentally competitive designs and approaches. Emerging concepts that are lagging in this respect can address their shortcomings by aiming to reach higher efficiencies, longer lifetimes, substituting novel materials, and/or reducing the energy intensive of their manufacturing processes.

To this end, two emerging and relevant aspects to further enhance the LCA evaluation for both technologies are represented by the new tendency of “greener” materials and processes, that can significantly influence the material, waste, and energy flows at the early stage of a device life cycle.

To date, most of the research efforts aim to develop new organic and hybrid semiconductors with improved performance. However, less attention is paid on their environmental profile. Indeed, most synthetic strategies currently used to prepare these systems are demanding from both raw materials/chemical costs and environmental point of view, and their large-scale production may present serious limitations. Therefore, the development of waste minimized and clean synthetic methodologies where minimal amounts of reagents, reaction media, solid catalysts, and solvents (for reactions and purifications) are used, or the replacement of critical and/or toxic components/elements, such in the case of PSCs,^[268] is of crucial importance for the scalability of the material production. For instance, the application of principles of green chemistry, or similar concepts related to short steps of synthesis, inexpensive, and with high yields, for the development of waste minimized and clean synthetic approaches to semiconductor synthesis is essential for the field of organic/hybrid electronics.^[269] This is one of the biggest challenges for the practical application of PSCs considering the relatively short durability of perovskite materials and corresponding devices, even though many kinds of strategies have been proposed to improve PSCs operational stability (Juarez-Perez and Haro, 2020).

Concerning OSCs, an interesting study was carried out by Po et al.,^[270] ranking active-layer donor polymers according to a figure of merit based on synthetic complexity (including the number of synthetic steps, yields, amount of solvents, and safety characteristics of chemicals/solvents) and PCE, and providing some guidelines for the rational design of green and efficient

materials. This clearly proved that tailored materials can potentially break the current efficiency record, but complex solutions are doomed to remain confined to the world of research.

The second relevant aspect is related to the eco-friendly processing (with “green” solvents) of PV devices.^[271] Often, laboratory-scale hero cells are processed from hazardous, toxic, and expensive chlorinated solvents that are not the best choice in view of a sustainable large-scale production. The scientific community is, therefore, working to find green solvents suitable for an ecofriendly device processing. It means not only to test different solvents on available materials, but also to tune the chemical structure of the materials, when possible, to improve the solubility in a broad range of solvents, such as unchlorinated and nonaromatic, or in a more specific solvent such as water. For example, an environmentally friendly 2-methyltetrahydrofuran, derived from renewable natural resources such as corncobs and bagasse, was used for the fabrication of high-performance OSCs with PCEs exceeding 10%.^[272] Other green solvents have also been used for highly efficient OSCs,^[38,273] also highlighting benefits from the stability point of view.^[274]

4.3. Cost Figures

Before a technology is commercialized, it needs to be economically evaluated to test whether it meets the requirements of the market competition. Specifically, the total system cost is divided by the amount of electricity that can be generated during the life time of OSCs, and ultimately, the cost per unit of electricity is obtained, which is widely called leveled electricity cost (LEC; \$ kWh⁻¹). The economic evaluation includes the material cost, production cost, and process cost of the PV module, module cost, and PV system operating cost. Recent research efforts have been targeted to the economic evaluation of the OSC marketization. In 2011, Nelson showed that if the efficiency of large-area modules can reach about 7%, and the life span can reach at least five years, then OSCs could achieve competitive power output comparing with silicon solar cells.^[275] An LEC of between 0.22\$ and 0.59\$ kWh⁻¹ was calculated using the P3HT/PCBM system under an average solar irradiance of 1700 kWh m⁻² year⁻¹.^[275] Min et al. made a cost analysis of fully solution-processed organic solar modules in 2019. It was found that the price of raw materials accounts for 75% of manufacturing costs. Hence, in upscaling and industrial scenarios, a lower module cost could be realized by the significant reduction in the price of raw materials and electrode. LEC values range from 0.185 to 0.486¥ kWh⁻¹ (0.027–0.072\$ kWh⁻¹) have been estimated for OSCs with 10% PCE, with an average of 0.324¥ kWh⁻¹ (0.048\$ kWh⁻¹) under an average solar irradiance of 1200 kWh m⁻² year⁻¹, if a lifetime of ten years is achieved.^[28] Furthermore, it was found that the LEC value based on the same assumptions reduces to 0.102¥ kWh⁻¹ (0.015\$ kWh⁻¹) in the middle of Australia and Chile with very sufficient sunlight. Li and co-workers indicated that the active materials of OSCs are generally expensive due to their complicated synthetic process and low yield.^[276] Thus, the exploration of novel low-cost materials and their related processing technology is particularly urgent. It is believed that with the further improvements of the efficiency of OSC devices and the continuous reduction of manufacturing costs of modules

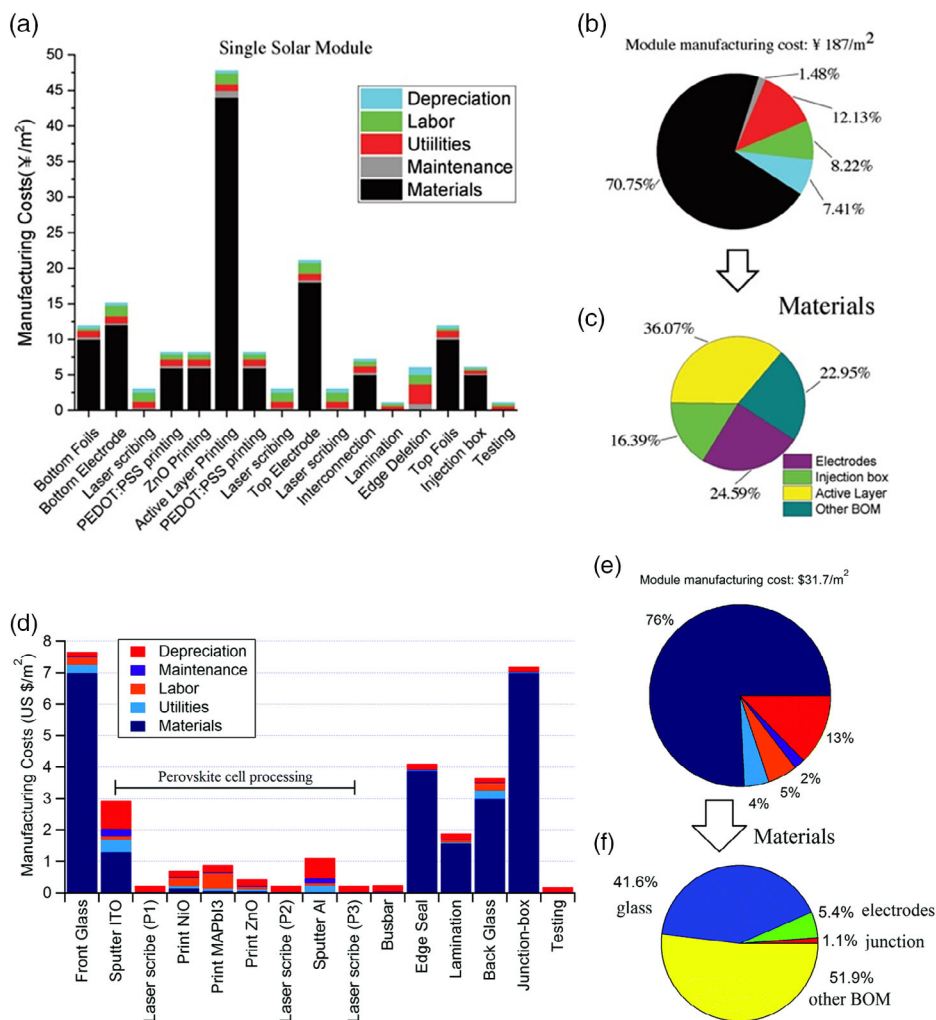


Figure 11. a) Manufacturing cost of organic solar modules. b) Direct module manufacturing cost distribution. c) Material costs. Reproduced with permission.^[294] Copyright 2018, Wiley-VCH. d) Step-by-step direct manufacturing costs of the reference monolithic perovskite PV module. e) Direct manufacturing cost distribution. f) Materials cost breakdown of the reference module with a total manufacturing cost of \$31.7 per m². Reproduced with permission.^[279] Copyright 2017, The Royal Society of Chemistry.

(mainly materials' costs), the LEC value will drop to a lower level, which will give OSC more advantages in the energy market (Figure 11).

Although the PCE of laboratory-scale PSCs has achieved a certified 25.5%, it is difficult to realize a high PCE of the large-scale PSCs modules, because PCE decreases with the increasing device area due to the nonuniformity of device fabrication, structure defects, larger ohmic losses, and loss of active area from interconnection.^[277] Cai et al. analyzed the cost of PSC modules on the basis of the lifetime of 15 years.^[278] The results show that the leveled cost of electricity of a PSCs module is 0.049, 0.042, and 0.035 \$ kWh⁻¹ on 12%, 15%, and 20%, respectively. By comparison, the cost for traditional energy sources is 0.0704–0.0119 \$ kWh⁻¹, and commercialized solar PVs are 0.0978–0.1933 \$ kWh⁻¹.

With the development of the material science, more and more high efficiency of PSCs using lower cost materials has been reported in the literature. This cost might be overestimated

due to the use of high price materials. Heben et al. assessed the cost of perovskite modules by putting more attention on manufacturable module configuration produced in an actual in-line industry plant. It is estimated that the direct manufacturing cost was 31.7 \$ m⁻², and a leveled cost of energy was 0.0493–0.0790 \$ kWh⁻¹ with the module operating at 16% PCE in a 30 years cycle.^[279] Thus, the minimum required conversion efficiency of PSCs should meet the following key target: the cost of the electricity from the PSCs modules should be less than that from the commercial PV modules at the set PCE and years. For the raw materials, the primary attention should be paid on low cost, availability, and environmental friendliness. For the large-scale materials preparation, the focus should be on the reduction and optimization of the synthetic steps, also minimizing waste, costs, and environmental impact. To date, besides material and device stability issues, the large-scale material preparation represents a big challenge for the practical application of PSCs.

4.4. SWOT Analysis

The promotion and diffusion of new PV technologies depend on several interrelated factors, from basic scientific aspects to socio-economic considerations.^[280] As outlined earlier, quantitative metrics have been developed to estimate the energy performance of PVs technologies in different environments, related to realistic operation conditions.^[281,282] However, a general evaluation of the technology, in view of a strategic planning of possible implementation approaches, can be provided by the strengths, weaknesses, opportunities, and threats (SWOT) analysis.^[283] This approach has been pursued especially to assess the potential of generic PV technologies in the context of specific geographical and local areas, considering the balance between scientific/industrial aspects and real societal and economic advantages.^[284–286] Here, we perform a SWOT analysis focused on the potential impact of OSC and PSC technologies from the point of view of industrial scaling-up. The analysis is conducted by collecting relevant data and information from the literature considered in the previous sections and summarizing the main aspects related to the evaluation of SWOT factors in a qualitative comparison between OSCs and PSCs. The main findings can be summarized as follows.

4.4.1. Organic Solar Cells

Strengths: 1) The nature of materials used (organic molecules and polymers) allows solution-based fabrication methods and, thus, enables the possibility of translating laboratory-scale techniques to the fabrication of large-area modules with relatively small efforts; 2) material tenability; tailored for applications; 3) fabrication methods meet the requirements of high-throughput R2R techniques; 4) devices can be: flexible, lightweight, colored, and transparent; 5) high sensitivity to low light conditions; 6) higher PCE under low light conditions and/or diffused/indirect illumination (e.g., indoor) compared with conventional technologies; and 7) low environmental impact; no toxic elements/materials.

Weaknesses: 1) The price of raw materials for the fabrication of devices can be high; 2) the PCE, measured under standard illumination, is still lower compared with other technologies; and 3) the use of organic materials can lead to reduced working lifetimes under harsh conditions.

Opportunities: 1) The peculiarities of OPV technologies can make them the most suitable choice for less energy-intensive application scenarios, such as wearable devices and domestic electricity consumption; 2) development of new materials to overcome intrinsic losses of OSCs; and 3) development of material with low synthetic complexity and/or synthetic methods to reduce costs and environmental impact.

Threats: Other emerging PV technologies, including PSCs, can overcome the main limitations of OSCs.

4.4.2. Perovskite Solar Cells

Strength: 1) The fabrication technology of PSCs is compatible with R2R and other high-throughput manufacturing methods, pointing to a strong potential for industrial scale-up. 2) The

PCE obtained in modules based on PSC is remarkably high with respect to other technologies. 3) Methods for the deposition/fabrication of perovskite materials require low energies.

Weaknesses: 1) The nature of materials used in PSCs leads to durability issues. 2) The great variability of materials used, fabrication processes, and device architectures in PSCs leads to significant difficulties in the development of standards for assessing performance and lifetime of solar cells, with a strong impact on the industrial uptake of the technology. 3) The use of lead perovskites as basic photoactive materials in PSCs leads to significant issues related to materials toxicity and life cycle of devices.

Opportunities: 1) There is still room for improving the PCE of PSCs based on lead-free materials (for example, tin perovskites). 2) Technological advancements in the fabrication process can enhance the PCE of solar cells modules. 3) Development of synthesis and fabrication routes based on low-cost raw materials can lead to highly efficient and economically convenient PSCs. 4) Routes for recycling all components of PSCs can be developed.

Threats: 1) The lifetime of PSCs is still lagging behind that of available PV modules. 2) The large-scale adoption of PSC technologies can lead to significant environmental issues, related to the use of lead in the perovskite materials (**Figure 12**).

5. Conclusion and Outlook

In this work, we reviewed the recent progress in the development of OSC and PSC technologies in view of their potential in real setting applications. The analysis of the basic principles of working mechanisms and architecture, the crucial role of materials design, synthesis, and modeling, and the progress in the translation of laboratory-scale methods toward industrial large-scale production allowed us to outline a comparative assessment of the two main emerging technologies for next-generation solar cells.

Both technologies display a wide range of distinct properties, which can be exploited in different application scenarios. Rather than deciding a unique winner that would be able to beat the competition in all aspects related to solar energy harvesting, recent research demonstrates that a wide number of applications can profit from the peculiarities of both OSC and PSC technologies, respectively.

The potential of PV technologies in real use-case settings is largely related to the power density of the energy source from which light is actually harvested and converted into electricity. The perhaps most interesting and most engaging application scenario concerns the realization of large solar cell modules for power-intensive harvesting of sunlight. Although still dominated by traditional silicon-based technologies, current research efforts are striving to assess the potential of PSCs as alternative, low-cost, and high-efficiency technologies in the realization of solar cell farms.

Nevertheless, novel PVs technologies can also be used for other outdoor applications. The lower theoretical efficiency of OSCs, which is related to the excitonic dissociation processes, is compensated by other advantages. The spectrum of possibilities offered by the manifold of materials that can potentially be used for fabricating efficient OPV devices opens new

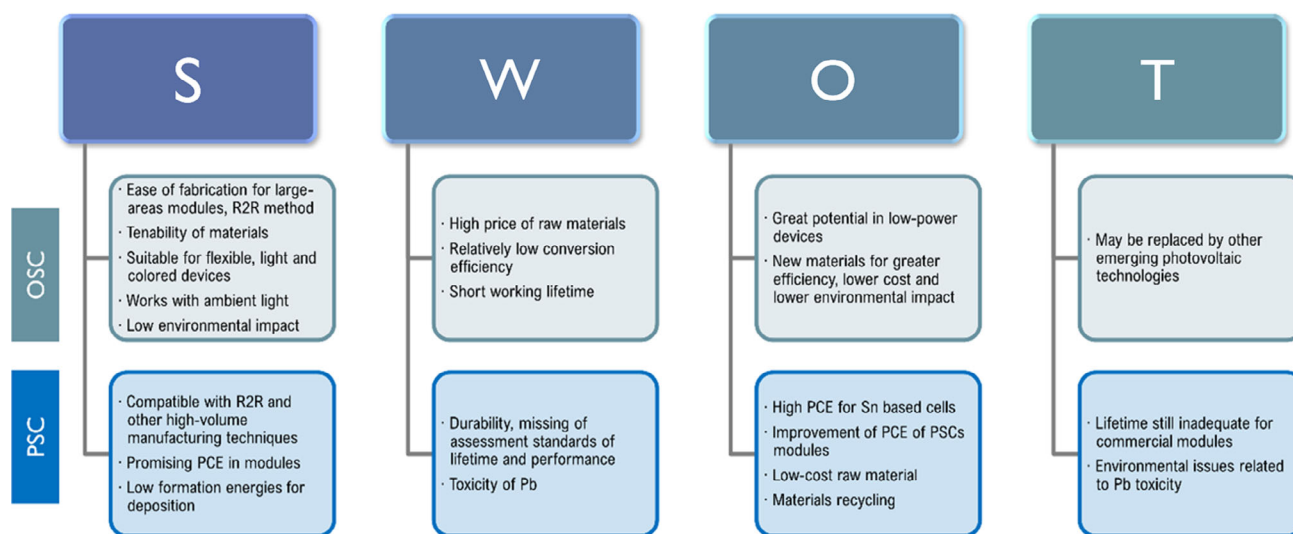


Figure 12. Schematics of the SWOT analysis for the real setting applications of OSC and PSC technologies.

perspectives for a wide set of target applications. For example, the integration of PV modules into architectural and structural components of buildings (building-integrated PVs [BIPV]), where relatively low efficiencies can be accepted, also sets some other constraints (transparency, color, and flexibility) that can make OSC the technology of choice.^[287] In this respect, however, very recent work has also demonstrated the potential of PSCs in this field of application.^[288]

OSCs and PSCs can also outperform other PV systems in indoor applications and for harvesting ambient light. In these applications, the relatively low power produced by PV devices can still be extremely useful for reducing the use of batteries, also with a significant environmental impact at the large scale. An emerging advantage in using novel PV technologies to harvest ambient light is related to the intensity and the spectrum of innovative lighting sources, such as LEDs and organic light emitting diodes. PSCs and OSCs can exhibit a better fraction of energy recycled from light sources with respect, for example, to silicon-based cells. This behavior can be ascribed to the larger overlap between the emission spectrum of the light source and the absorption spectrum of the photoactive layers in PSCs or OSCs with respect to other platforms and can ultimately be related to the physicochemical affinity between materials used in the light-emitting and -absorbing devices, respectively.

The low-weight and flexibility of thin-film OSCs and PSCs can also find application in the development of consumer appliances (watches, sensors, home digital devices, wearable devices, smart textiles, and small displays). Integrated low-power PV systems are also often used in connection with devices powered by rechargeable batteries. Although OSCs have generally been proposed for this kind of applications, recent work also highlights the possibility of using thin-film PSCs for flexible devices.^[289]

Another potentially disruptive application of OSC and PSC technologies concerns the development of devices for health care and medicine. Besides the possibility of developing self-powered medical devices, PV platforms can supply electrical power to biosensors or implants or to other bioelectronic devices. In

particular, the demand of efficient devices for bioelectronics (from lab-on-chip systems to neural and brain-machine interfaces) is currently growing at a fast pace, with a significant impact on future market opportunities in the field. A relevant property required for the application of PV platforms in this field is a wide and tunable absorption spectrum (from NIR to VIS), needed to match the requirement of specific applications. These fields of application, however, also pose stringent requirements for the biocompatibility of PV platforms. From this point of view, OSCs can offer a wider set of opportunities with respect to PSCs.

Furthermore, an emerging field of application of innovative PV technologies is that of low-power energy sources for Internet of Things (IoT) devices. The IoT technology is expected to rapidly boost in the next few years, with an estimate of about 75 billion devices worldwide expected by 2025. Most of these devices will operate under ambient light, thus matching the optimal working conditions for OSCs and PSCs. Clearly, the possibility of replacing batteries with integrated PV platforms opens new opportunities for the development of IoT technologies. Recently, thin-film PSCs have been used as energy sources for radio-frequency identification (RFID) systems,^[290] and work is in progress to extend this approach to other IoT platforms.

Overall, the OSC and PSC technologies are in the stage of finding their path to initial market proposition building on their specificity and strength with respect to existing products. The faith of both technologies for large-scale market uptake still relies on the output of dedicated research and development activities to solve blocking issues and make the products economically competitive and sustainable.

Acknowledgements

M.S. and F.M. contributed equally to this work.

Conflict of Interest

The authors declare no conflict of interest.

Keywords

comparative review, organic solar cells, perovskite solar cells, real setting applications

Received: October 14, 2020

Revised: February 28, 2021

Published online: April 10, 2021

- [1] N. Armaroli, V. Balzani, *Chem. – A Eur. J.* **2016**, *22*, 32.
- [2] G. C. Righini, F. Enrichi, in *Solar Cells and Light Management* (Eds.: F. Enrichi, G. C. Righini), Elsevier, Amsterdam **2020**, pp. 1–32.
- [3] S. Dubey, N. Y. Jadhav, B. Zakirova, *Energy Procedia* **2013**, *33*, 322.
- [4] EUChemS, *Elements' Scarcity Periodic Table*, **2019**.
- [5] Q. Liu, Y. Zhang, Y. Wang, W. Wang, C. Gu, S. Huang, H. Yuan, O. P. Dhankher, *J. Hazard. Mater.* **2020**, *400*, 123165.
- [6] J. Yan, B. R. Saunders, *RSC Adv.* **2014**, *4*, 43286.
- [7] P. Müller-Buschbaum, M. Thelakkat, T. F. Fässler, M. Stutzmann, *Adv. Energy Mater.* **2017**, *7*, 1700248.
- [8] A. Mishra, P. Bäuerle, in *Organic Photovoltaics*, Wiley-VCH Verlag GmbH & Co. KGaA, Weinheim, Germany **2014**, pp. 139–170.
- [9] A. Venkateswararao, K.-T. Wong, *Bull. Chem. Soc. Jpn.* **2021**, *94*, 812.
- [10] <https://www.heliotech.com> (accessed: June 2020).
- [11] A. Chilvery, S. Das, P. Guggilla, C. Brantley, A. Sunda-Meya, *Sci. Technol. Adv. Mater.* **2016**, *17*, 650.
- [12] F.-C. Chen, *Adv. Opt. Mater.* **2019**, *7*, 1800662.
- [13] J. S. Manser, J. A. Christians, P. V. Kamat, *Chem. Rev.* **2016**, *116*, 12956.
- [14] A. J. Heeger, *Chem. Soc. Rev.* **2010**, *39*, 2354.
- [15] O. Inganäs, *Adv. Mater.* **2018**, *30*, 1800388.
- [16] C. L. Cutting, M. Bag, D. Venkataraman, *J. Mater. Chem. C* **2016**, *4*, 10367.
- [17] R. R. Søndergaard, N. Espinosa, M. Jørgensen, F. C. Krebs, *Energy Environ. Sci.* **2014**, *7*, 1006.
- [18] D. Hengevoss, C. Baumgartner, G. Nisato, C. Hugi, *Sol. Energy* **2016**, *137*, 317.
- [19] W. R. Mateker, M. D. McGehee, *Adv. Mater.* **2017**, *29*, 1603940.
- [20] H. Kallmann, M. Pope, *J. Chem. Phys.* **1959**, *30*, 585.
- [21] C. W. Tang, *Appl. Phys. Lett.* **1986**, *48*, 183.
- [22] G. Yu, J. Gao, J. C. Hummelen, F. Wudl, A. J. Heeger, *Science* **1995**, *270*, 1789.
- [23] J. J. M. Halls, C. A. Walsh, N. C. Greenham, E. A. Marseglia, R. H. Friend, S. C. Moratti, A. B. Holmes, *Nature* **1995**, *376*, 498.
- [24] S. Morita, A. A. Zakhidov, K. Yoshino, *Solid State Commun.* **1992**, *82*, 249.
- [25] N. S. Sariciftci, L. Smilowitz, A. J. Heeger, F. Wudl, *Science* **1992**, *258*, 1474.
- [26] K. Wang, C. Liu, T. Meng, C. Yi, X. Gong, *Chem. Soc. Rev.* **2016**, *45*, 2937.
- [27] Q. An, F. Zhang, J. Zhang, W. Tang, Z. Deng, B. Hu, *Energy Environ. Sci.* **2016**, *9*, 281.
- [28] D. Di Carlo Rasi, R. A. J. Janssen, *Adv. Mater.* **2019**, *31*, 1806499.
- [29] M. Prosa, M. Tassarolo, M. Bolognesi, T. Cramer, Z. Chen, A. Facchetti, B. Fraboni, M. Seri, G. Ruani, M. Muccini, *Adv. Mater. Interfaces* **2016**, *3*, 1600770.
- [30] P. W. M. Blom, V. D. Mihailetschi, L. J. A. Koster, D. E. Markov, *Adv. Mater.* **2007**, *19*, 1551.
- [31] A. Moliton, J. M. Nunzi, *Polym. Int.* **2006**, *55*, 583.
- [32] C. M. Proctor, M. Kuik, T. Q. Nguyen, *Prog. Polym. Sci.* **2013**, *38*, 1941.
- [33] Q. Liu, Y. Jiang, K. Jin, J. Qin, J. Xu, W. Li, J. Xiong, J. Liu, Z. Xiao, K. Sun, S. Yang, X. Zhang, L. Ding, *Sci. Bull.* **2020**, *65*, 272.
- [34] J. E. Carlé, M. Helgesen, O. Hagemann, M. Hösel, I. M. Heckler, E. Bundgaard, S. A. Gevorgyan, R. R. Søndergaard, M. Jørgensen, R. García-Valverde, S. Chaouki-Almagro, J. A. Villarejo, F. C. Krebs, *Joule* **2017**, *1*, 274.
- [35] S. Hong, H. Kang, G. Kim, S. Lee, S. Kim, J. H. Lee, J. Lee, M. Yi, J. Kim, H. Back, J. R. Kim, K. Lee, *Nat. Commun.* **2016**, *7*, 10279.
- [36] T. Zhang, G. Zeng, F. Ye, X. Zhao, X. Yang, *Adv. Energy Mater.* **2018**, *8*, 1801387.
- [37] S. Mori, H. Oh-Oka, H. Nakao, T. Gotanda, Y. Nakano, H. Jung, A. Iida, R. Hayase, N. Shida, M. Saito, K. Todori, T. Asakura, A. Matsui, M. Hosoya, *Mater. Res. Soc. Symp. Proc.* **2015**, *1737*, 26.
- [38] C.-Y. Liao, Y.-K. Y. Chen, C.-H. C.-C. Lee, G. Wang, N.-W. Teng, C.-H. C.-C. Lee, W.-L. Li, Y.-K. Y. Chen, C.-H. Li, H.-L. Ho, P. H.-S. Tan, B. Wang, Y.-C. Huang, R. M. Young, M. R. Wasielewski, T. J. Marks, Y.-M. Chang, A. Facchetti, *Joule* **2020**, *4*, 189.
- [39] C.-Y. Tsai, Y.-H. Lin, Y.-M. Chang, J.-C. Kao, Y.-C. Liang, C.-C. Liu, J. Qiu, L. Wu, C.-Y. Liao, H.-S. Tan, Y.-C. Chao, S.-F. Horng, H.-W. Zan, H.-F. Meng, F. Li, *Sol. Energy Mater. Sol. Cells* **2020**, *218*, 110762.
- [40] P. Cheng, X. Zhan, *Chem. Soc. Rev.* **2016**, *45*, 2544.
- [41] X. Du, T. Heumueller, W. Gruber, A. Classen, T. Unruh, N. Li, C. J. Brabec, *Joule* **2019**, *3*, 215.
- [42] Q. Burlingame, X. Huang, X. Liu, C. Jeong, C. Coburn, S. R. Forrest, *Nature* **2019**, *573*, 394.
- [43] NREL, *Champion Photovoltaic Module Efficiency Chart*, <https://www.nrel.gov/pv/module-efficiency.html> (accessed: September 2020).
- [44] X. Zhang, H. Liu, W. Wang, J. Zhang, B. Xu, K. L. Karen, Y. Zheng, S. Liu, S. Chen, K. Wang, X. W. Sun, *Adv. Mater.* **2017**, *29*, 1606405.
- [45] A. Miyata, A. Mitioglu, P. Plochocka, O. Portugall, J. T. W. Wang, S. D. Stranks, H. J. Snaith, R. J. Nicholas, *Nat. Phys.* **2015**, *11*, 582.
- [46] L. R. V. Buizza, T. W. Crothers, Z. Wang, J. B. Patel, R. L. Milot, H. J. Snaith, M. B. Johnston, L. M. Herz, *Adv. Funct. Mater.* **2019**, *29*, 1902656.
- [47] B. Bahrami, A. H. Chowdhury, A. Gurung, S. Mabrouk, K. M. Reza, S. I. Rahman, R. Pathak, Q. Qiao, *Nano Today* **2020**, *33*, 100874.
- [48] I. E. Castelli, J. M. García-Lastra, K. S. Thygesen, K. W. Jacobsen, *APL Mater.* **2014**, *2*, 081514.
- [49] J. N. Wilson, J. M. Frost, S. K. Wallace, A. Walsh, *APL Mater.* **2019**, *7*, 010901.
- [50] M. A. Green, A. Ho-Baillie, H. J. Snaith, *Nat. Photonics* **2014**, *8*, 506.
- [51] A. Amat, E. Mosconi, E. Ronca, C. Quarti, P. Umari, M. K. Nazeeruddin, M. Grätzel, F. De Angelis, *Nano Lett.* **2014**, *14*, 3608.
- [52] F. Zheng, L. Z. Tan, S. Liu, A. M. Rappe, *Nano Lett.* **2015**, *15*, 7794.
- [53] J. M. Frost, *Phys. Rev. B* **2017**, *96*, 195202.
- [54] T. Ivanovska, C. Quarti, G. Grancini, A. Petrozza, F. De Angelis, A. Milani, G. Ruani, *ChemSusChem* **2016**, *9*, 2994.
- [55] C. W. Myung, J. Yun, G. Lee, K. S. Kim, *Adv. Energy Mater.* **2018**, *8*, 1702898.
- [56] T. Zhao, W. Shi, J. Xi, D. Wang, Z. Shuai, *Sci. Rep.* **2016**, *7*, 19968.
- [57] C. Liu, H. Tsai, W. Nie, D. J. Gosztola, X. Zhang, *J. Phys. Chem. Lett.* **2020**, *11*, 6256.
- [58] D. Meggiolaro, F. Ambrosio, E. Mosconi, A. Mahata, F. De Angelis, *Adv. Energy Mater.* **2020**, *10*, 1902748.
- [59] L. Qiao, W.-H. Fang, R. Long, O. V. Prezhdo, *J. Phys. Chem. Lett.* **2020**, *11*, 7066.
- [60] L. Wang, N. P. Brawand, M. Vörös, P. D. Dahlberg, J. P. Otto, N. E. Williams, D. M. Tiede, G. Galli, G. S. Engel, *Adv. Opt. Mater.* **2018**, *6*, 1700975.
- [61] W. P. D. Wong, J. Yin, B. Chaudhary, X. Y. Chin, D. Cortecchia, S.-Z. A. Lo, A. C. Grimsdale, O. F. Mohammed, G. Lanzani, C. Soci, *ACS Mater. Lett.* **2020**, *2*, 20.

- [62] F. Zheng, L. Wang, *Energy Environ. Sci.* **2019**, *12*, 1219.
- [63] H. Zhu, M. T. Trinh, J. Wang, Y. Fu, P. P. Joshi, K. Miyata, S. Jin, X.-Y. Zhu, *Adv. Mater.* **2017**, *29*, 1603072.
- [64] D. Ghosh, E. Welch, A. J. Neukirch, A. Zakhidov, S. Tretiak, *J. Phys. Chem. Lett.* **2020**, *11*, 3271.
- [65] T. Ivanovska, C. Dionigi, E. Mosconi, F. De Angelis, F. Liscio, V. Morandi, G. Ruani, *J. Phys. Chem. Lett.* **2017**, *8*, 3081.
- [66] M. M. Lee, J. Teuscher, T. Miyasaka, T. N. Murakami, H. J. Snaith, *Science* **2012**, *338*, 643.
- [67] N. J. Jeon, J. H. Noh, Y. C. Kim, W. S. Yang, S. Ryu, S. Il Seok, *Nat. Mater.* **2014**, *13*, 897.
- [68] N. Rolston, K. A. Bush, A. D. Printz, A. Gold-Parker, Y. Ding, M. F. Toney, M. D. McGehee, R. H. Dauskardt, *Adv. Energy Mater.* **2018**, *8*, 1802139.
- [69] J. Burschka, N. Pellet, S. J. Moon, R. Humphry-Baker, P. Gao, M. K. Nazeeruddin, M. Grätzel, *Nature* **2013**, *499*, 316.
- [70] C. Bi, Y. Shao, Y. Yuan, Z. Xiao, C. Wang, Y. Gao, J. Huang, *J. Mater. Chem. A* **2014**, *2*, 18508.
- [71] C. Momblona, O. Malinkiewicz, C. Roldán-Carmona, A. Soriano, L. Gil-Escrig, E. Bandiello, M. Scheepers, E. Edri, H. J. Bolink, *APL Mater.* **2014**, *2*, 081504.
- [72] N.-G. Park, *Nano Converg.* **2016**, *3*, 15.
- [73] J. H. Im, C. R. Lee, J. W. Lee, S. W. Park, N. G. Park, *Nanoscale* **2011**, *3*, 4088.
- [74] J. Y. Jeng, Y. F. Chiang, M. H. Lee, S. R. Peng, T. F. Guo, P. Chen, T. C. Wen, *Adv. Mater.* **2013**, *25*, 3727.
- [75] HZB, *World Record: Efficiency of Perovskite Silicon Tandem Solar Cell Jumps to 29.15 per cent*, <https://www.nrel.gov/pv/cell-efficiency.html> (accessed: January 2021).
- [76] Y. H. Lin, N. Sakai, P. Da, J. Wu, H. C. Sansom, A. J. Ramadan, S. Mahesh, J. Liu, R. D. J. Oliver, J. Lim, L. Aspirtarte, K. Sharma, P. K. Madhu, A. B. Morales-Vilches, P. K. Nayak, S. Bai, F. Gao, C. R. M. Grovenor, M. B. Johnston, J. G. Labram, J. R. Durrant, J. M. Ball, B. Wenger, B. Stannowski, H. J. Snaith, *Science* **2020**, *369*, 96.
- [77] A. Al-Ashouri, E. Köhnen, B. Li, A. Magomedov, H. Hempel, P. Caprioglio, J. A. Márquez, A. B. Morales Vilches, E. Kasparavicius, J. A. Smith, N. Phung, D. Menzel, M. Grischek, L. Kegelmann, D. Skroblin, C. Gollwitzer, T. Malinauskas, M. Jošt, G. Matič, B. Rech, R. Schlattmann, M. Topič, L. Korte, A. Abate, B. Stannowski, D. Neher, M. Stollerfoht, T. Unold, V. Getautis, S. Albrecht, *Science* **2020**, *370*, 1300.
- [78] NEDO New Energy and Industrial Technology Development Organization, *Japan's NEDO And Panasonic Achieve The World's Highest Conversion Efficiency Of 16.09% For Largest-Area Perovskite Solar Cell Module*, https://www.nedo.go.jp/english/news/AA5en_100421.html (accessed: February 2020).
- [79] H. Lu, Y. Liu, P. Ahlwat, A. Mishra, W. R. Tress, F. T. Eickemeyer, Y. Yang, F. Fu, Z. Wang, C. E. Avalos, B. I. Carlsen, A. Agarwalla, X. Zhang, X. Li, Y. Zhan, S. M. Zakeeruddin, L. Emsley, U. Rothlisberger, L. Zheng, A. Hagfeldt, M. Grätzel, *Science* **2020**, *370*, eabb8985.
- [80] C. C. Boyd, R. Cheacharoen, T. Leijtens, M. D. McGehee, *Chem. Rev.* **2019**, *119*, 3418.
- [81] N. Pellet, P. Gao, G. Gregori, T. Y. Yang, M. K. Nazeeruddin, J. Maier, M. Grätzel, *Angew. Chem., Int. Ed.* **2014**, *53*, 3151.
- [82] C. C. Stoumpos, C. D. Malliakas, M. G. Kanatzidis, *Inorg. Chem.* **2013**, *52*, 9019.
- [83] Y. Han, H. Zhao, C. Duan, S. Yang, Z. Yang, Z. Liu, S. Liu, *Adv. Funct. Mater.* **2020**, *30*, 1909972.
- [84] G. Grancini, C. Roldán-Carmona, I. Zimmermann, E. Mosconi, X. Lee, D. Martineau, S. Narbey, F. Oswald, F. De Angelis, M. Graetzel, M. K. Nazeeruddin, *Nat. Commun.* **2017**, *8*, 15684.
- [85] Y. Feng, Q. Hu, E. Rezaee, M. Li, Z. X. Xu, A. Lorenzoni, F. Mercuri, M. Muccini, *Adv. Energy Mater.* **2019**, *9*, 1901019.
- [86] X. Zhou, W. Qi, J. Li, J. Cheng, Y. Li, J. Luo, M. J. Ko, Y. Li, Y. Zhao, X. Zhang, *Sol. RRL* **2020**, *4*, 2000308.
- [87] P. Boonmongkolras, D. Kim, E. M. Alhabshi, I. Gereige, B. Shin, *RSC Adv.* **2018**, *8*, 21551.
- [88] A. Polman, M. Knight, E. C. Garnett, B. Ehrler, W. C. Sinke, *Science* **2016**, *352*, aad4424.
- [89] S. Almosni, A. Delamarre, Z. Jehl, D. Suchet, L. Cojocaru, M. Giteau, B. Behaghel, A. Julian, C. Ibrahim, L. Taty, H. Wang, T. Kubo, S. Uchida, H. Segawa, N. Miyashita, R. Tamaki, Y. Shoji, K. Yoshida, N. Ahsan, K. Watanabe, T. Inoue, M. Sugiyama, Y. Nakano, T. Hamamura, T. Toupance, C. Olivier, S. Chambon, L. Vignau, C. Geffroy, E. Cloutet, et al., *Sci. Technol. Adv. Mater.* **2018**, *19*, 336.
- [90] A. Facchetti, *Chem. Mater.* **2011**, *23*, 733.
- [91] H. S. Jung, N.-G. Park, *Small* **2015**, *11*, 10.
- [92] Q. Yue, W. Liu, X. Zhu, *J. Am. Chem. Soc.* **2020**, *142*, 11613.
- [93] E. M. Tennyson, T. A. S. Doherty, S. D. Stranks, *Nat. Rev. Mater.* **2019**, *4*, 573.
- [94] W. Deng, X. Liang, P. S. Kubiak, P. J. Cameron, *Adv. Energy Mater.* **2018**, *8*, 1701544.
- [95] T.-H. Lai, S.-W. Tsang, J. R. Manders, S. Chen, F. So, *Mater. Today* **2013**, *16*, 424.
- [96] W. W. H. Wong, J. L. Banal, P. B. Geraghty, Q. Hong, B. Zhang, A. B. Holmes, D. J. Jones, *Chem. Rec.* **2015**, *15*, 1006.
- [97] A. E. Shalan, *Mater. Adv.* **2020**, *1*, 292.
- [98] N. Asim, K. Sopian, S. Ahmadi, K. Saeedfar, M. A. Alghoul, O. Saadatian, S. H. Zaidi, *Renew. Sustain. Energy Rev.* **2012**, *16*, 5834.
- [99] J. Chen, N.-G. Park, *ACS Energy Lett.* **2020**, *5*, 2742.
- [100] N.-G. Park, *Trans. Electr. Electron. Mater.* **2020**, *21*, 1.
- [101] H. J. Son, F. He, B. Carsten, L. Yu, *J. Mater. Chem.* **2011**, *21*, 18934.
- [102] M. M. Wienk, J. M. Kroon, W. J. H. Verhees, J. Knol, J. C. Hummelen, P. A. van Hal, R. A. J. Janssen, *Angew. Chem., Int. Ed.* **2003**, *42*, 3371.
- [103] P. Schilinsky, C. Waldauf, C. J. Brabec, *Appl. Phys. Lett.* **2002**, *81*, 3885.
- [104] F. Padinger, R. S. Rittberger, N. S. Sariciftci, *Adv. Funct. Mater.* **2003**, *13*, 85.
- [105] M. T. Dang, L. Hirsch, G. Wantz, J. D. Wuest, *Chem. Rev.* **2013**, *113*, 3734.
- [106] C. Yang, S. Zhang, J. Ren, M. Gao, P. Bi, L. Ye, J. Hou, *Energy Environ. Sci.* **2020**, *13*, 2864.
- [107] M. Leclerc, *J. Polym. Sci. Part A Polym. Chem.* **2001**, *39*, 2867.
- [108] M. Svensson, F. Zhang, S. C. Veenstra, W. J. H. Verhees, J. C. Hummelen, J. M. Kroon, O. Inganäs, M. R. Andersson, *Adv. Mater.* **2003**, *15*, 988.
- [109] L. H. Slooff, S. C. Veenstra, J. M. Kroon, D. J. D. Moet, J. Sweelssen, M. M. Koetse, *Appl. Phys. Lett.* **2007**, *90*, 143506.
- [110] L. Dou, Y. Liu, Z. Hong, G. Li, Y. Yang, *Chem. Rev.* **2015**, *115*, 12633.
- [111] Y.-J. Cheng, S.-H. Yang, C.-S. Hsu, *Chem. Rev.* **2009**, *109*, 5868.
- [112] G. Li, W.-H. Chang, Y. Yang, *Nat. Rev. Mater.* **2017**, *2*, 17043.
- [113] X. Gong, G. Li, C. Li, J. Zhang, Z. Bo, *J. Mater. Chem. A* **2015**, *3*, 20195.
- [114] D. Mühlbacher, M. Scharber, M. Morana, Z. Zhu, D. Waller, R. Gaudiana, C. Brabec, *Adv. Mater.* **2006**, *18*, 2931.
- [115] J. Peet, J. Y. Kim, N. E. Coates, W. L. Ma, D. Moses, A. J. Heeger, G. C. Bazan, *Nat. Mater.* **2007**, *6*, 497.
- [116] H.-Y. Chen, J. Hou, A. E. Hayden, H. Yang, K. N. Houk, Y. Yang, *Adv. Mater.* **2010**, *22*, 371.
- [117] J. S. J.-S. Kim, Z. Fei, S. Wood, D. T. James, M. Sim, K. Cho, M. J. Heeney, J. S. J.-S. Kim, *Adv. Energy Mater.* **2014**, *4*, 1400527.
- [118] L. Dou, C.-C. Chen, K. Yoshimura, K. Ohya, W.-H. Chang, J. Gao, Y. Liu, E. Richard, Y. Yang, *Macromolecules* **2013**, *46*, 3384.

- [119] Y. Liu, J. Zhao, Z. Li, C. Mu, W. Ma, H. Hu, K. Jiang, H. Lin, H. Ade, H. Yan, *Nat. Commun.* **2014**, *5*, 5293.
- [120] S. Qu, H. Tian, *Chem. Commun.* **2012**, *48*, 3039.
- [121] K. H. Hendriks, G. H. L. Heintges, V. S. Gevaerts, M. M. Wienk, R. A. J. Janssen, *Angew. Chem., Int. Ed.* **2013**, *52*, 8341.
- [122] L. Dou, J. You, J. Yang, C.-C. Chen, Y. He, S. Murase, T. Moriarty, K. Emery, G. Li, Y. Yang, *Nat. Photonics* **2012**, *6*, 180.
- [123] L. Dou, W.-H. Chang, J. Gao, C.-C. Chen, J. You, Y. Yang, *Adv. Mater.* **2013**, *25*, 825.
- [124] R. S. Ashraf, I. Meager, M. Nikolka, M. Kirkus, M. Planells, B. C. Schroeder, S. Holliday, M. Hurhangee, C. B. Nielsen, H. Sirringhaus, I. McCulloch, *J. Am. Chem. Soc.* **2015**, *137*, 1314.
- [125] Y. Liang, Z. Xu, J. Xia, S.-T. Tsai, Y. Wu, G. Li, C. Ray, L. Yu, *Adv. Mater.* **2010**, *22*, E135.
- [126] Y. Liang, Y. Wu, D. Feng, S.-T. Tsai, H.-J. Son, G. Li, L. Yu, *J. Am. Chem. Soc.* **2009**, *131*, 56.
- [127] J. Hou, M.-H. Park, S. Zhang, Y. Yao, L.-M. Chen, J.-H. Li, Y. Yang, *Macromolecules* **2008**, *41*, 6012.
- [128] Z. He, C. Zhong, S. Su, M. Xu, H. Wu, Y. Cao, *Nat. Photonics* **2012**, *6*, 591.
- [129] Z. He, B. Xiao, F. Liu, H. Wu, Y. Yang, S. Xiao, C. Wang, T. P. Russell, Y. Cao, *Nat. Photonics* **2015**, *9*, 174.
- [130] E. Wang, W. Mammo, M. R. Andersson, *Adv. Mater.* **2014**, *26*, 1801.
- [131] R. Stalder, J. Mei, J. R. Reynolds, *Macromolecules* **2010**, *43*, 8348.
- [132] D. Gedefaw, M. Prosa, M. Bolognesi, M. Seri, M. R. Andersson, *Adv. Energy Mater.* **2017**, *7*, 1700575.
- [133] D. Dang, W. Chen, R. Yang, W. Zhu, W. Mammo, E. Wang, *Chem. Commun.* **2013**, *49*, 9335.
- [134] L. Zhu, M. Wang, B. Li, C. Jiang, Q. Li, *J. Mater. Chem. A* **2016**, *4*, 16064.
- [135] B. Zheng, L. Huo, Y. Li, *NPG Asia Mater.* **2020**, *12*, 3.
- [136] Z. Zhou, W. Liu, G. Zhou, M. Zhang, D. Qian, J. Zhang, S. Chen, S. Xu, C. Yang, F. Gao, H. Zhu, F. Liu, X. Zhu, *Adv. Mater.* **2020**, *32*, 1906324.
- [137] X. Ma, J. Wang, J. Gao, Z. Hu, C. Xu, X. Zhang, F. Zhang, *Adv. Energy Mater.* **2020**, *10*, 2001404.
- [138] J. Cao, L. Qian, F. Lu, J. Zhang, Y. Feng, X. Qiu, H. L. Yip, L. Ding, *Chem. Commun.* **2015**, *51*, 11830.
- [139] M. An, F. Xie, X. Geng, J. Zhang, J. Jiang, Z. Lei, D. He, Z. Xiao, L. Ding, *Adv. Energy Mater.* **2017**, *7*, 1602509.
- [140] J. Xiong, K. Jin, Y. Jiang, J. Qin, T. Wang, J. Liu, Q. Liu, H. Peng, X. Li, A. Sun, X. Meng, L. Zhang, L. Liu, W. Li, Z. Fang, X. Jia, Z. Xiao, Y. Feng, X. Zhang, K. Sun, S. Yang, S. Shi, L. Ding, *Sci. Bull.* **2019**, *64*, 1573.
- [141] H. Schlaich, M. Muccini, J. Feldmann, H. Bässler, E. O. Göbel, R. Zamboni, C. Taliani, J. Erxmeyer, A. Weidinger, *Chem. Phys. Lett.* **1995**, *236*, 135.
- [142] Y. He, Y. Li, *Phys. Chem. Chem. Phys.* **2011**, *13*, 1970.
- [143] Y. He, H. Y. Chen, J. Hou, Y. Li, *J. Am. Chem. Soc.* **2010**, *132*, 5532.
- [144] J. Zhang, H. S. Tan, X. Guo, A. Facchetti, H. Yan, *Nat. Energy* **2018**, *3*, 720.
- [145] A. Wadsworth, M. Moser, A. Marks, M. S. Little, N. Gasparini, C. J. Brabec, D. Baran, I. McCulloch, *Chem. Soc. Rev.* **2019**, *48*, 1596.
- [146] C. Huang, S. Barlow, S. R. Marder, *J. Org. Chem.* **2011**, *76*, 2386.
- [147] M. Bolognesi, D. Gedefaw, M. Cavazzini, M. Catellani, M. R. Andersson, M. Muccini, E. Kozma, M. Seri, *New J. Chem.* **2018**, *42*, 18633.
- [148] P. Cheng, G. Li, X. Zhan, Y. Yang, *Nat. Photonics* **2018**, *12*, 131.
- [149] Y. Lin, J. Wang, Z.-G. Zhang, H. Bai, Y. Li, D. Zhu, X. Zhan, *Adv. Mater.* **2015**, *27*, 1170.
- [150] Z. Xiao, S. Yang, Z. Yang, J. Yang, H.-L. Yip, F. Zhang, F. He, T. Wang, J. Wang, Y. Yuan, H. Yang, M. Wang, L. Ding, *Adv. Mater.* **2019**, *31*, 1804790.
- [151] Z. Xiao, X. Jia, L. Ding, *Sci. Bull.* **2017**, *62*, 1562.
- [152] J. Yuan, Y. Zhang, L. Zhou, G. Zhang, H.-L. Yip, T.-K. Lau, X. Lu, C. Zhu, H. Peng, P. A. Johnson, M. Leclerc, Y. Cao, J. Ulanski, Y. Li, Y. Zou, *Joule* **2019**, *3*, 1140.
- [153] Z. Li, M. Yang, J.-S. Park, S.-H. Wei, J. J. Berry, K. Zhu, *Chem. Mater.* **2016**, *28*, 284.
- [154] A. Kojima, K. Teshima, Y. Shirai, T. Miyasaka, *J. Am. Chem. Soc.* **2009**, *131*, 6050.
- [155] N. Li, X. Niu, Q. Chen, H. Zhou, *Chem. Soc. Rev.* **2020**, *49*, 8235.
- [156] Y. Chen, Y. Sun, J. Peng, J. Tang, K. Zheng, Z. Liang, *Adv. Mater.* **2018**, *30*, 1703487.
- [157] J. H. Noh, S. H. Im, J. H. Heo, T. N. Mandal, S. Il Seok, *Nano Lett.* **2013**, *13*, 1764.
- [158] S. A. Kulkarni, T. Baikie, P. P. Boix, N. Yantara, N. Mathews, S. Mhaisalkar, *J. Mater. Chem. A* **2014**, *2*, 9221.
- [159] G. E. Eperon, S. D. Stranks, C. Menelaou, M. B. Johnston, L. M. Herz, H. J. Snaith, *Energy Environ. Sci.* **2014**, *7*, 982.
- [160] O. J. Weber, B. Charles, M. T. Weller, *J. Mater. Chem. A* **2016**, *4*, 15375.
- [161] A. Binek, F. C. Hanusch, P. Docampo, T. Bein, *J. Phys. Chem. Lett.* **2015**, *6*, 1249.
- [162] M. Saliba, T. Matsui, J.-Y. Seo, K. Domanski, J.-P. Correa-Baena, M. K. Nazeeruddin, S. M. Zakeeruddin, W. Tress, A. Abate, A. Hagfeldt, M. Grätzel, *Energy Environ. Sci.* **2016**, *9*, 1989.
- [163] N.-G. Park, M. Grätzel, T. Miyasaka, K. Zhu, K. Emery, *Nat. Energy* **2016**, *1*, 16152.
- [164] Z. Chen, J. J. Wang, Y. Ren, C. Yu, K. Shum, *Appl. Phys. Lett.* **2012**, *101*, 093901.
- [165] M. Kulbak, D. Cahen, G. Hodes, *J. Phys. Chem. Lett.* **2015**, *6*, 2452.
- [166] J. K. Nam, S. U. Choi, W. Cha, Y. J. Choi, W. Kim, M. S. Jung, J. Kwon, D. Kim, J. H. Park, *Nano Lett.* **2017**, *17*, 2028.
- [167] C.-Y. Chen, H.-Y. Lin, K.-M. Chiang, W.-L. Tsai, Y.-C. Huang, C.-S. Tsao, H.-W. Lin, *Adv. Mater.* **2017**, *29*, 1605290.
- [168] Y. Wang, X. Liu, T. Zhang, X. Wang, M. Kan, J. Shi, Y. Zhao, *Angew. Chem., Int. Ed.* **2019**, *58*, 16691.
- [169] C. Liu, W. Li, J. Chen, J. Fan, Y. Mai, R. E. I. Schropp, *Nano Energy* **2017**, *41*, 75.
- [170] N. Kawano, M. Koshimizu, K. Asai, *J. Phys. Chem. C* **2012**, *116*, 22992.
- [171] H. Zhou, Q. Chen, G. Li, S. Luo, T.-b. Song, H.-S. Duan, Z. Hong, J. You, Y. Liu, Y. Yang, *Science* **2014**, *345*, 542.
- [172] S. Y. Park, J. S. Park, B. J. Kim, H. Lee, A. Walsh, K. Zhu, D. H. Kim, H. S. Jung, *Nat. Sustain.* **2020**, *3*, 1044.
- [173] M. Ghasemi, L. Zhang, J. Yun, M. Hao, D. He, P. Chen, Y. Bai, T. Lin, M. Xiao, A. Du, M. Lyu, L. Wang, *Adv. Funct. Mater.* **2020**, *30*, 2002342.
- [174] F. Igbari, R. Wang, Z.-K. Wang, X.-J. Ma, Q. Wang, K.-L. Wang, Y. Zhang, L.-S. Liao, Y. Yang, *Nano Lett.* **2019**, *19*, 2066.
- [175] M. Pantaler, K. T. Cho, V. I. E. Queloz, I. García Benito, C. Fettkenhauer, I. Anusca, M. K. Nazeeruddin, D. C. Lupascu, G. Grancini, *ACS Energy Lett.* **2018**, *3*, 1781.
- [176] W. Ning, F. Wang, B. Wu, J. Lu, Z. Yan, X. Liu, Y. Tao, J. M. Liu, W. Huang, M. Fahlman, L. Hultman, T. C. Sum, F. Gao, *Adv. Mater.* **2018**, *30*, 1706246.
- [177] H.-L. Yip, A. K.-Y. Jen, *Energy Environ. Sci.* **2012**, *5*, 5994.
- [178] Z. Yin, J. Wei, Q. Zheng, *Adv. Sci.* **2016**, *3*, 1500362.
- [179] W. Zhang, Y.-C. Wang, X. Li, C. Song, L. Wan, K. Usman, J. Fang, *Adv. Sci.* **2018**, *5*, 1800159.
- [180] S. Ben Dkhil, D. Duché, M. Gaceur, A. K. Thakur, F. B. Aboura, L. Escoubas, J.-J. Simon, A. Guerrero, J. Bisquet, G. Garcia-Belmonte, Q. Bao, M. Fahlman, C. Vidolot-Ackermann, O. Margeat, J. Ackermann, *Adv. Energy Mater.* **2014**, *4*, 1400805.

- [181] M. Bolognesi, M. Tassarolo, T. Posati, M. Nocchetti, V. Benfenati, M. Seri, G. Ruani, M. Muccini, *Org. Photonics Photovoltaics* **2013**, 1, 1.
- [182] X. Yu, T. J. Marks, A. Facchetti, *Nat. Mater.* **2016**, 15, 383.
- [183] M. Prosa, M. Tassarolo, M. Bolognesi, O. Margeat, D. Gedefaw, M. Gaceur, C. Vidolot-Ackermann, M. R. Andersson, M. Muccini, M. Seri, J. Ackermann, *ACS Appl. Mater. Interfaces* **2016**, 8, 1635.
- [184] Z. He, H. Wu, Y. Cao, *Adv. Mater.* **2014**, 26, 1006.
- [185] Y. Zhou, C. Fuentes-Hernandez, J. Shim, J. Meyer, A. J. Giordano, H. Li, P. Winget, T. Papadopoulos, H. Cheun, J. Kim, M. Fenoll, A. Dindar, W. Haske, E. Najafabadi, T. M. Khan, H. Sojoudi, S. Barlow, S. Graham, J.-L. Brédas, S. R. Marder, A. Kahn, B. Kippelen, *Science* **2012**, 336, 327.
- [186] A. Tada, Y. Geng, M. Nakamura, Q. Wei, K. Hashimoto, K. Tajima, *Phys. Chem. Chem. Phys.* **2012**, 14, 3713.
- [187] B. Roth, G. A. dos Reis Benatto, M. Corazza, R. R. Søndergaard, S. A. Gevorgyan, M. Jørgensen, F. C. Krebs, *Adv. Energy Mater.* **2015**, 5, 1401912.
- [188] T. Stubhan, N. Li, N. A. Luechinger, S. C. Halim, G. J. Matt, C. J. Brabec, *Adv. Energy Mater.* **2012**, 2, 1433.
- [189] Y. Hou, X. Du, S. Scheiner, D. P. McMeekin, Z. Wang, N. Li, M. S. Killian, H. Chen, M. Richter, I. Levchuk, N. Schrenker, E. Spiecker, T. Stubhan, N. A. Luechinger, A. Hirsch, P. Schmuki, H.-P. Steinrück, R. H. Fink, M. Halik, H. J. Snaith, C. J. Brabec, *Science* **2017**, 358, 1192.
- [190] K. Mahmood, S. Sarwar, M. T. Mehran, *RSC Adv.* **2017**, 7, 17044.
- [191] L. Xiong, Y. Guo, J. Wen, H. Liu, G. Yang, P. Qin, G. Fang, *Adv. Funct. Mater.* **2018**, 28, 1802757.
- [192] Z. H. Bakr, Q. Wali, A. Fakharuddin, L. Schmidt-Mende, T. M. Brown, R. Jose, *Nano Energy* **2017**, 34, 271.
- [193] W. Ke, P. Priyanka, S. Vegiraju, C. C. Stoumpos, I. Spanopoulos, C. M. M. Soe, T. J. Marks, M.-C. Chen, M. G. Kanatzidis, *J. Am. Chem. Soc.* **2018**, 140, 388.
- [194] P. Kung, M. Li, P. Lin, Y. Chiang, C. Chan, T. Guo, P. Chen, *Adv. Mater. Interfaces* **2018**, 5, 1800882.
- [195] M. Bidikoudi, E. Kymakis, *J. Mater. Chem. C* **2019**, 7, 13680.
- [196] E. Rezaee, X. Liu, Q. Hu, L. Dong, Q. Chen, J.-H. Pan, Z.-X. Xu, *Sol. RRL* **2018**, 2, 1800200.
- [197] U. Ahmed, M. Alizadeh, N. A. Rahim, S. Shahabuddin, M. S. Ahmed, A. K. Pandey, *A Comprehensive Review on Counter Electrodes for Dye Sensitized Solar Cells: A Special Focus on Pt-TCO Free Counter Electrodes*, Vol. 174, **2018**, pp. 1097–1125.
- [198] Y. Zhang, S.-W. Ng, X. Lu, Z. Zheng, *Chem. Rev.* **2020**, 120, 2049.
- [199] D. J. Burke, D. J. Lipomi, *Energy Environ. Sci.* **2013**, 6, 2053.
- [200] F. Yang, J. Liu, Z. Lu, P. Dai, T. Nakamura, S. Wang, L. Chen, A. Wakamiya, K. Matsuda, *Adv. Sci.* **2020**, 7, 1902474.
- [201] M.-G. Kang, M.-S. Kim, J. Kim, L. J. Guo, *Adv. Mater.* **2008**, 20, 4408.
- [202] Y. Djaoued, Vu Hong Phong, S. Badilescu, P. V. Ashrit, F. E. Girouard, Vo-Van Truong, *Thin Solid Films* **1997**, 293, 108.
- [203] D. S. Hecht, L. Hu, G. Irvin, *Adv. Mater.* **2011**, 23, 1482.
- [204] F. Mercuri, M. Baldoni, A. Sgamellotti, *Nanoscale* **2012**, 4, 369.
- [205] D. Selli, M. Baldoni, A. Sgamellotti, F. Mercuri, *Nanoscale* **2012**, 4, 1350.
- [206] X. Wang, L. Zhi, N. Tsao, Ž. Tomović, J. Li, K. Müllen, *Angew. Chemie Int. Ed.* **2008**, 47, 2990.
- [207] J. Nelson, *The Physics of Solar Cells*, Imperial College Press/World Scientific Publishing Co., London **2003**.
- [208] W. Shockley, H. J. Queisser, *J. Appl. Phys.* **1961**, 32, 510.
- [209] A. Kumar, *J. Appl. Phys.* **2017**, 121, 014502.
- [210] J. Hou, O. Inganäs, R. H. Friend, F. Gao, *Nat. Mater.* **2018**, 17, 119.
- [211] M. Auf der Maur, M. Povolotskiy, F. Sacconi, G. Romano, E. Petrolati, A. Di Carlo, in *Simulation of Semiconductor Processes and Devices*, Springer Vienna, Vienna, **2007**, pp. 245–248.
- [212] M. Auf Der Maur, G. Penazzi, G. Romano, F. Sacconi, A. Pecchia, A. Di Carlo, *IEEE Trans. Electron Devices* **2011**, 58, 1425.
- [213] A. Lorenzoni, *PhD Thesis*, University of Bologna, **2018**.
- [214] D. Beljonne, J. Cornil, in *Multiscale Modelling of Organic and Hybrid Photovoltaics* in D. Beljonne, J. Cornil (Eds.), Vol. 352, Springer Berlin Heidelberg, Berlin, Heidelberg **2014**.
- [215] C.-K. Lee, C.-W. Pao, C.-W. Chu, *Energy Environ. Sci.* **2011**, 4, 4124.
- [216] A. Lorenzoni, M. Baldoni, E. Besley, F. Mercuri, *Phys. Chem. Chem. Phys.* **2020**, 22, 12482.
- [217] M. F. Horstemeyer, in *Practical Aspects of Computational Chemistry*, Springer Netherlands, Dordrecht **2009**, pp. 87–135.
- [218] Q. H. Zeng, A. B. Yu, G. Q. Lu, *Multiscale Modeling and Simulation of Polymer Nanocomposites*, Vol. 33, **2008**, pp. 191–269.
- [219] G. Fitzgerald, J. Dejoannis, M. Meunier, in *Modeling, Characterization, and Production of Nanomaterials*, Elsevier, Amsterdam **2015**, pp. 3–53.
- [220] B. C. Barnes, J. K. Brennan, E. F. C. Byrd, S. Izvekov, J. P. Larentzos, B. M. Rice, in *Computational Approaches for Chemistry Under Extreme Conditions. Challenges and Advances in Computational Chemistry and Physics*, Vol. 28 (Ed.: N. Goldman), Springer, Cham **2019**.
- [221] M. Baldoni, A. Lorenzoni, A. Pecchia, F. Mercuri, *Phys. Chem. Chem. Phys.* **2018**, 20, 28393.
- [222] J. D. Lee, J. Li, Z. Zhang, L. Wang, in *Micromechanics and Nanomechanics of Composite Solids*, Springer International Publishing, Cham **2018**, pp. 1–38.
- [223] N. Martinelli, Y. Olivier, L. Muccioli, A. Minoia, P. Brocorens, M.-C. R. Delgado, C. Zannoni, D. Beljonne, R. Lazzaroni, J.-L. Brédas, J. Cornil, in *Functional Supramolecular Architectures*, WILEY-VCH Verlag & Co. KGaA, Weinheim, Germany **2014**, pp. 1–38.
- [224] D. L. Cheung, A. Troisi, *Phys. Chem. Chem. Phys.* **2008**, 10, 5941.
- [225] A. Lorenzoni, M. Muccini, F. Mercuri, *RSC Adv.* **2015**, 5, 11797.
- [226] A. Lorenzoni, M. Muccini, F. Mercuri, *J. Phys. Chem. C* **2017**, 121, 21857.
- [227] A. Lorenzoni, F. Gallino, M. Muccini, F. Mercuri, *RSC Adv.* **2016**, 6, 40724.
- [228] A. B. Walker, *Proc. IEEE* **2009**, 97, 1587.
- [229] M. Pippig, F. Mercuri, *J. Chem. Phys.* **2020**, 152, 164102.
- [230] S. Alowayyed, T. Piontek, J. L. Suter, O. Hoenen, D. Groen, O. Luk, B. Bosak, P. Kopta, K. Kurowski, O. Perks, K. Brabazon, V. Jancauskas, D. Coster, P. V. Coveney, A. G. Hoekstra, *Futur. Gener. Comput. Syst.* **2019**, 91, 335.
- [231] Y. Wu, J. Guo, R. Sun, J. Min, *NPJ Comput. Mater.* **2020**, 6, 120.
- [232] W. Sun, Y. Zheng, K. Yang, Q. Zhang, A. A. Shah, Z. Wu, Y. Sun, L. Feng, D. Chen, Z. Xiao, S. Lu, Y. Li, K. Sun, *Sci. Adv.* **2019**, 5, eaay4275.
- [233] J. Zhang, H.-B. Li, S.-L. Sun, Y. Geng, Y. Wu, Z.-M. Su, *J. Mater. Chem.* **2012**, 22, 568.
- [234] M. K. Nazeeruddin, F. De Angelis, S. Fantacci, A. Selloni, G. Viscardi, P. Liska, S. Ito, B. Takeru, M. Grätzel, *J. Am. Chem. Soc.* **2005**, 127, 16835.
- [235] S. Mathew, A. Yella, P. Gao, R. Humphry-Baker, B. F. E. Curchod, N. Ashari-Astani, I. Tavernelli, U. Rothlisberger, M. K. Nazeeruddin, M. Grätzel, *Nat. Chem.* **2014**, 6, 242.
- [236] N. Blouin, A. Michaud, D. Gendron, S. Wakim, E. Blair, R. Neagu-Plesu, M. Belletête, G. Durocher, Y. Tao, M. Leclerc, *J. Am. Chem. Soc.* **2008**, 130, 732.
- [237] A. Zhugayevych, O. Postupna, R. C. Bakus II, G. C. Welch, G. C. Bazan, S. Tretiak, *J. Phys. Chem. C* **2013**, 117, 4920.
- [238] A. Lorenzoni, A. Mosca Conte, A. Pecchia, F. Mercuri, *Nanoscale* **2018**, 10, 9376.
- [239] A. Lorenzoni, M. Muccini, F. Mercuri, *Adv. Theory Simulations* **2019**, 2, 1900156.

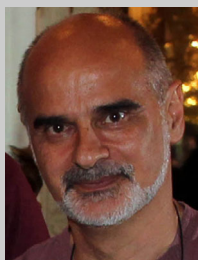
- [240] A. M. A. Leguy, J. M. Frost, A. P. McMahon, V. G. Sakai, W. Kockelmann, C. Law, X. Li, F. Foglia, A. Walsh, B. C. O'Regan, J. Nelson, J. T. Cabral, P. R. F. Barnes, *Nat. Commun.* **2015**, *6*, 7124.
- [241] D. Bartesaghi, I. D. C. Pérez, J. Kniepert, S. Roland, M. Turbiez, D. Neher, L. J. A. Koster, *Nat. Commun.* **2015**, *6*, 7083.
- [242] W. Tress, K. Leo, M. Riede, *Adv. Funct. Mater.* **2011**, *21*, 2140.
- [243] H. Mäckel, R. C. I. MacKenzie, *Phys. Rev. Appl.* **2018**, *9*, 034020.
- [244] Y. Firdaus, V. M. Le Corre, J. I. Khan, Z. Kan, F. Laquai, P. M. Beaujuge, T. D. Anthopoulos, *Adv. Sci.* **2019**, *6*, 1802028.
- [245] X. Ren, Z. Wang, W. E. I. Sha, W. C. H. Choy, *ACS Photonics* **2017**, *4*, 934.
- [246] M. G. Villalva, J. R. Gazoli, E. R. Filho, *IEEE Trans. Power Electron.* **2009**, *24*, 1198.
- [247] M. Sajedi Alvar, P. W. M. Blom, G.-J. A. H. Wetzelaer, *Nat. Commun.* **2020**, *11*, 4023.
- [248] Y. Tong, Z. Xiao, X. Du, C. Zuo, Y. Li, M. Lv, Y. Yuan, C. Yi, F. Hao, Y. Hua, T. Lei, Q. Lin, K. Sun, D. Zhao, C. Duan, X. Shao, W. Li, H. L. Yip, Z. Xiao, B. Zhang, Q. Bian, Y. Cheng, S. Liu, M. Cheng, Z. Jin, S. Yang, L. Ding, *Sci. China Chem.* **2020**, *63*, 758.
www.solarcellcentral.com.
- [250] R. Abbel, Y. Galagan, P. Groen, *Adv. Eng. Mater.* **2018**, *20*, 1701190.
- [251] L. Lucera, P. Kubis, F. W. Fecher, C. Bronnbauer, M. Turbiez, K. Forberich, T. Ameri, H. J. Egelhaaf, C. J. Brabec, *Energy Technol.* **2015**, *3*, 373.
- [252] Q. Wang, Y. Xie, F. Soltani-Kordshuli, M. Eslamian, *Renew. Sustain. Energy Rev.* **2016**, *56*, 347.
- [253] T. R. Andersen, H. F. Dam, M. Hösel, M. Helgesen, J. E. Carlé, T. T. Larsen-Olsen, S. A. Gevorgyan, J. W. Andreasen, J. Adams, N. Li, F. Machui, G. D. Spyropoulos, T. Ameri, N. Lemaître, M. Legros, A. Scheel, D. Gaiser, K. Kreul, S. Berny, O. R. Lozman, S. Nordman, M. Välimäki, M. Vilkmann, R. R. Søndergaard, M. Jørgensen, C. J. Brabec, F. C. Krebs, *Energy Environ. Sci.* **2014**, *7*, 2925.
- [254] S. K. Karunakaran, G. M. Arumugam, W. Yang, S. Ge, S. N. Khan, X. Lin, G. Yang, *J. Mater. Chem. A* **2019**, *7*, 13873.
- [255] G. Wang, M. A. Adil, J. Zhang, Z. Wei, *Adv. Mater.* **2019**, *31*, 1805089.
- [256] T. M. Schmidt, T. T. Larsen-Olsen, J. E. Carlé, D. Angmo, F. C. Krebs, *Adv. Energy Mater.* **2015**, *5*, 1500569.
- [257] X. Liu, X. Guo, Y. Lv, Y. Hu, J. Lin, Y. Fan, N. Zhang, X. Liu, *ACS Appl. Mater. Interfaces* **2018**, *10*, 18141.
- [258] S. Berny, N. Blouin, A. Distler, H.-J. Egelhaaf, M. Krompiec, A. Lohr, O. R. Lozman, G. E. Morse, L. Nanson, A. Pron, T. Saueremann, N. Seidler, S. Tierney, P. Tiwana, M. Wagner, H. Wilson, *Adv. Sci.* **2016**, *3*, 1500342.
- [259] Y. Zhang, I. D. W. Samuel, T. Wang, D. G. Lidzey, *Adv. Sci.* **2018**, *5*, 1800434.
- [260] A. M. Freitas, R. A. M. Gomes, R. A. M. Ferreira, M. P. Porto, *Renew. Energy* **2019**, *135*, 1004.
- [261] J. Ahmad, K. Bazaka, L. J. Anderson, R. D. White, M. V. Jacob, *Renewable Sustainable Energy Rev.* **2013**, *27*, 104.
- [262] A. Uddin, M. Upama, H. Yi, L. Duan, *Coatings* **2019**, *9*, 65.
- [263] H. Kimura, K. Fukuda, H. Jinno, S. Park, M. Saito, I. Osaka, K. Takimiya, S. Umezumi, T. Someya, *Adv. Mater.* **2019**, *31*, 1808033.
- [264] T. Yokota, P. Zalar, M. Kaltenbrunner, H. Jinno, N. Matsuhisa, H. Kitanosako, Y. Tachibana, W. Yukita, M. Koizumi, T. Someya, *Sci. Adv.* **2016**, *2*, e1501856.
- [265] T. Ibn-Mohammed, S. C. L. Koh, I. M. Reaney, A. Acquaye, G. Schileo, K. B. Mustapha, R. Greenough, *Renewable Sustainable Energy Rev.* **2017**, *80*, 1321.
- [266] V. Muteri, M. Cellura, D. Curto, V. Franzitta, S. Longo, M. Mistretta, M. L. Parisi, *Energies* **2020**, *13*, 252.
- [267] C. F. Blanco, S. Cucurachi, W. J. G. M. Peijnenburg, A. Beames, M. G. Vijver, *Energy Technol.* **2020**, *8*, 1901064.
- [268] G. Nasti, A. Abate, *Adv. Energy Mater.* **2020**, *10*, 1902467.
- [269] A. Marrocchi, A. Facchetti, D. Lanari, C. Petrucci, L. Vaccaro, *Energy Environ. Sci.* **2016**, *9*, 763.
- [270] R. Po, G. Bianchi, C. Carbonera, A. Pellegrino, *Macromolecules* **2015**, *48*, 453.
- [271] S. Zhang, L. Ye, H. Zhang, J. Hou, *Mater. Today* **2016**, *19*, 533.
- [272] Z. Li, L. Ying, P. Zhu, W. Zhong, N. Li, F. Liu, F. Huang, Y. Cao, *Energy Environ. Sci.* **2019**, *12*, 157.
- [273] L. Hong, H. Yao, Z. Wu, Y. Cui, T. Zhang, Y. Xu, R. Yu, Q. Liao, B. Gao, K. Xian, H. Y. Woo, Z. Ge, J. Hou, *Adv. Mater.* **2019**, *31*, 1903441.
- [274] M. Bolognesi, M. Prosa, M. Tassarolo, G. Donati, S. Toffanin, M. Muccini, M. Seri, *Sol. Energy Mater. Sol. Cells* **2016**, *155*, 436.
- [275] B. Azzopardi, C. J. M. Emmott, A. Urbina, F. C. Krebs, J. Mutale, J. Nelson, *Energy Environ. Sci.* **2011**, *4*, 3741.
- [276] R. Xue, J. Zhang, Y. Li, Y. Li, *Small* **2018**, *14*, 1801793.
- [277] I. Celik, Z. Song, A. J. Cimaroli, Y. Yan, M. J. Heben, D. Apul, *Sol. Energy Mater. Sol. Cells* **2016**, *156*, 157.
- [278] M. Cai, Y. Wu, H. Chen, X. Yang, Y. Qiang, L. Han, *Adv. Sci.* **2017**, *4*, 1600269.
- [279] Z. Song, C. L. McElvany, A. B. Phillips, I. Celik, P. W. Krantz, S. C. Wathage, G. K. Liyanage, D. Apul, M. J. Heben, *Energy Environ. Sci.* **2017**, *10*, 1297.
- [280] K. Reinsberger, T. Bruderer, S. Hatzl, E. Fleiß, A. Posch, *Appl. Energy* **2015**, *159*, 178.
- [281] A. M. Gracia-Amillo, G. Bardizza, E. Salis, T. Huld, E. D. Dunlop, *Energy-based Metric for Analysis of Organic PV Devices in Comparison with Conventional Industrial Technologies*, Vol. **93**, **2018**, pp. 76–89.
- [282] A. Urbina, *J. Phys. Energy* **2020**, *2*, 022001.
- [283] H. Wehrich, *Long Range Plann.* **1982**, *15*, 54.
- [284] F. Dinçer, *Renewable Sustainable Energy Rev.* **2011**, *15*, 3768.
- [285] H. M. Liou, *Renewable Sustainable Energy Rev.* **2010**, *14*, 1202.
- [286] J. Hou, H. Wang, P. Liu, *Int. J. Energy Res.* **2018**, *42*, 2050.
- [287] C. Toledo, R. López-Vicente, J. Abad, A. Urbina, *Energy Build.* **2020**, *223*, 110087.
- [288] H. Wang, H. A. Dewi, T. M. Koh, A. Bruno, S. Mhaisalkar, N. Mathews, *ACS Appl. Mater. Interfaces* **2020**, *12*, 484.
- [289] S. A. Hashemi, S. Ramakrishna, A. G. Aberle, *Recent Progress in Flexible-Wearable Solar Cells for Self-Powered Electronic Devices*, Vol. **13**, **2020**, pp. 685–743.
- [290] I. Mathews, S. N. R. Kantareddy, S. Sun, M. Layurova, J. Thapa, J. Correa-Baena, R. Bhattacharyya, T. Buonassisi, S. Sarma, I. M. Peters, *Adv. Funct. Mater.* **2019**, *29*, 1904072.
- [291] A. K. Jena, A. Kulkarni, T. Miyasaka, *Chem. Rev.* **2019**, *119*, 3036.
- [292] C. Eames, J. M. Frost, P. R. F. Barnes, B. C. O'Regan, A. Walsh, M. S. Islam, *Nat. Commun.* **2015**, *6*, 7497.
- [293] T. Abu Hamed, N. Adamovic, U. Aeberhard, D. Alonso-Alvarez, Z. Amin-Akhlagh, M. Auf der Maur, N. Beattie, N. Bednar, K. Berland, S. Birner, M. Califano, I. Capan, B. Cerne, I. Chilibon, J. P. Connolly, F. Cortes Juan, J. Coutinho, C. David, K. Deppert, V. Donchev, M. Drev, B. Ehlen, N. Ekins-Daukes, J. Even, L. Fara, D. Fournes Marron, A. Gagliardi, B. Garrido, V. Gianneta, M. Gomes, et al., *EPJ Photovoltaics* **2018**, *9*, 10.
- [294] J. Guo, J. Min, *A Cost Analysis of Fully Solution-Processed ITO-Free Organic Solar Modules*, Vol. **9**, **2019**, p. 1802521.
- [295] <http://www.sunflower-fp7.eu/index.php/opv-technology/demonstration-kit.html> (accessed: February 2021).
- [296] <https://sauletech.com/product/> (accessed: February 2021).



Mirko Seri is a chemist and received his Ph.D. degree in chemistry at the University of Perugia, Italy. Part of his research activity was carried out at Northwestern University, and then he moved to Consiglio Nazionale delle Ricerche (CNR), where he started to work on organic optoelectronic devices. His research interest includes solution-processable polymer solar cells with particular attention to the structure–property relationship of active/functional materials and device optimization for the fabrication of scalable single- or multijunction devices.



Francesco Mercuri received his M.Sc. degree in chemistry and his Ph.D. degree from the University of Perugia, Italy, in 1995 and 2000, respectively, in collaboration with the Max-Planck-Institut Stuttgart, Germany. He has been a staff and a guest scientist at the ETH-Zurich/Manno, Switzerland, École Nationale Supérieure de Chimie de Paris, France, University of Oxford, UK, Max-Planck-Institut and TU Dresden, Germany, and several others. He is currently a senior researcher at the Institute for Nanostructured Materials of the Italian National Research Council (CNR-ISMN). His research interests include multiscale modeling, HPC, and artificial intelligence.



Giampiero Ruani is a physicist, research director at the Institute for Nanostructured Materials of the Italian National Research Council (CNR-ISMN). His research interests spans from basic research on condensed matter to the applications of novel materials in renewable energies, optoelectronics and spintronics.



Yaomiao Feng is a research assistant in the Chemistry Department of South University of Science and Technology of China. His research is focused on organic semiconductors synthesis and applications in new energy harvesting, such as perovskite solar cells.



Minzhang Li is Ph.D. candidate in the Chemistry Department of South University of Science and Technology of China. His research is focused on phthalocyanine synthesis and application in new energy storage, such as supercapacitors.



Zong-Xiang Xu is an associate professor in the Chemistry Department of South University of Science and Technology of China since 2012. In 2008, he received a Ph.D. degree in chemistry from the University of Hong Kong and then joined the City University of Hong Kong, where he completed postdoctoral research between 2010 and 2012. Currently, his research is focused on molecular materials design and its applications in new energy harvesting, such as perovskite solar cells.



Michele Muccini is a director of the Institute for Nanostructured Materials of the Italian National Research Council (CNR-ISMN) and the President of the public–private industrial consortium MISTER Smart Innovation. His research interests and activity span from advanced materials, organic photonics, bioelectronics, and functional optoelectronic devices for a variety of application fields, including energy, health, and sustainability. Muccini has been a founder and a managing director of a start-up in the field of advanced optoelectronics.